Fall 2021

Fabrication of silicon nitride parts by ceramic on-demand extrusion process

Sachin Choudhary

Department:

FABRICATION OF SILICON NITRIDE PARTS BY CERAMIC ON-DEMAND EXTRUSION PROCESS

by

SACHIN CHOUDHARY

A THESIS

Presented to the Graduate Faculty of the

MISSOURI UNIVERSITY OF SCIENCE AND TECHNOLOGY

In Partial Fulfillment of the Requirements for the Degree

MASTER OF SCIENCE

in

MECHANICAL ENGINEERING

2021

Approved by:

Ming Leu, Advisor
Greg Hilmas
Jeremy Watts
David Bayless

PUBLICATION DISSERTATION OPTION

This dissertation contains the following article, formatted in the style used by the Missouri University of Science and Technology.

Paper I, found on pages 2–38 has been submitted to International Journal of Applied Ceramic Technology.

ABSTRACT

Ceramic On-Demand Extrusion (CODE) is a patented solid freeform fabrication method for manufacturing high-density monolithic ceramic parts. In the past 5-6 years, the technology has been successfully implemented to fabricate alumina and zirconia parts. The mechanical characterizations also show CODE's high potential in achieving desired structural properties. The present study covers the fabrication of silicon nitride parts by CODE process, which entailed the design of paste formulation for achieving rheology suitable for dimensional control in fabricated parts and determining firing temperature and the content of sintering additives for silicon nitride green bodies fabricated by CODE. The density, hardness, and fracture toughness measurements showed comparable properties achieved against other additive manufacturing processes. The microstructure and XRD data confirmed the full densification achieved in the sintered samples. Demonstration samples with and without support material were successfully fabricated by the CODE process. During the research, the user guidelines for the CODE process and process control model were described for better transfer of technology and identifying areas needing further exploration for achieving process excellence[1].

---

[1] **HONEYWELL FEDERAL MANUFACTURING & TECHNOLOGIES, LLC OPERATES THE KANSAS CITY NATIONAL SECURITY CAMPUS FOR THE UNITED STATES DEPARTMENT OF ENERGY / NATIONAL NUCLEAR SECURITY ADMINISTRATION UNDER CONTRACT NUMBER DE-NA0002839**

ACKNOWLEDGMENTS

I express my gratitude to Prof. Ming C. Leu for allowing me to be a part of the research, for his feedback on my work, and for supporting me during the most testing time of my life. I express my gratitude and respect to the Department of Energy's Office, Kansas City National Security Campus, managed by Honeywell, for the research assistantship. I want to thank Prof. Gregory E. Hilmas for his encouragement at every stage of my study and research. I cannot thank Prof. Jeremy Watts enough for his constant help and guidance on various aspects of research and experiments. Thanks to Dr. David Bayless for his support and for being part of my advisory committee. I am thankful to all members of the CODE Research Group with whom I got an opportunity to work, especially Benjamin Kroehler, Wenbin Li, Nathan Heaton, Krishna, Sha, Hossein, Austin Sutton & Robert and Austin Martin for all the help and inspiration. I fondly remember few fellow graduate students from the material science group, especially Paul & Alec for their compassionate behavior and help during lab work. I am grateful to friends, campus staff, and a few people from the campus & Rolla community for their tremendous support and help. Finally, I devote my work to my parents Anand Choudhary and Neelam Choudhary, as my whole existence is only because of them and their sacrifices.

TABLE OF CONTENTS

Page

PUBLICATION DISSERTATION OPTION iii

ABSTRACT iv

ACKNOWLEDGMENTS v

LIST OF ILLUSTRATIONS ix

LIST OF TABLES x

NOMENCLATURE xi

SECTION

1. INTRODUCTION 1

PAPER

I. FABRICATION OF HIGHLY DENSE SILICON NITRIDE PARTS BY CERAMIC ON-DEMAND EXTRUSION PROCESS AND PRESSURELESS SINTERING 2

ABSTRACT 2

1. INTRODUCTION 3

2. EXPERIMENTAL PROCEDURE 7

2.1. STARTING POWDERS AND ORGANIC CONSTITUENTS 7

2.2. ZETA POTENTIAL ANALYSIS 8

2.3. SINTERING AID CONTENT AND DENSIFICATION 9

2.4. BINDER CONTENT 9

2.5. PREPARATION OF PASTE FOR CODE PROCESS 10

2.6. RHEOLOGICAL CHARACTERIZATION 11

2.7. THERMOGRAVIMETRIC ANALYSIS (TGA)..... 12

2.8. PART FABRICATION BY CODE PROCESS..... 12

2.9. DENSIFICATION STUDY PROCEDURE..... 14

2.10. HARDNESS & FRACTURE TOUGHNESS MEASUREMENT PROCEDURE..... 15

3. RESULTS..... 15

3.1. CHARACTERIZATION OF POWDERS & SLURRIES..... 15

3.2. RHEOLOGICAL CHARACTERIZATION..... 17

3.3. BINDER BURNOUT..... 20

3.4. ADDITIVE CONTENT AND SINTERING TEMPERATURE..... 22

3.5. FABRICATION AND FIRING FOR DENSITY CHARACTERIZATION..... 25

3.6. DENSITY CHARACTERIZATION..... 25

3.7. HARDNESS & FRACTURE TOUGHNESS..... 26

3.8. MICROSTRUCTURE OF FABRICATED SILICON NITRIDE PARTS..... 28

3.9. XRD (X-RAY DIFFRACTION) ANALYSIS..... 29

3.10. CODE FABRICATED SILICON NITRIDE PARTS..... 31

3.11. COMPARISON WITH OTHER MANUFACTURING PROCESSES..... 32

4. CONCLUSION..... 33

ACKNOWLEDGEMENT..... 34

REFERENCES..... 35

SECTION

2. CONCLUSIONS AND RECOMMENDATIONS..... 39

2.1. CONCLUSIONS..... 39

2.2. RECOMMENDATIONS 40

APPENDIX……...…….41

VITA……..……46

LIST OF ILLUSTRATIONS

PAPER I Page

Figure 1. Setup for the Ceramic On-Demand Extrusion process..... 12

Figure 2. Raster spacing concept depiction 14

Figure 3. Zeta potential measurements for silicon nitride formulation powder mix. 16

Figure 4. Zeta profile for different dispersants for silicon nitride. 17

Figure 5. Variation of yield stress in silicon nitride-based CODE formulation with binder content..... 18

Figure 6. Viscosity profiles of silicon nitride formulation. 19

Figure 7. G' and G" for silicon nitride formulation (Table 4) at room temperature..... 20

Figure 8. TGA curves for determining binder burnout cycle for the 50 vol% silicon nitride paste formulation. 21

Figure 9. Sintering cycle for silicon nitride parts fabricated by CODE process in 0.1 MPa nitrogen gas environment. 22

Figure 10. Densities in silicon nitride specimens at a nozzle travel speed of 310 mm/min..... 24

Figure 11. As-printed silicon nitride billets (above), sintered silicon nitride billets (below). 25

Figure 12. Hardness indentation in polished silicon nitride sample (left), Vickers's indentation for evaluating fracture toughness (right). 28

Figure 13. Microstructure for sintered silicon nitride samples. 29

Figure 14. XRD (X-ray Diffraction) pattern analysis of silicon nitride powder mix. 30

Figure 15. XRD pattern of sintered silicon nitride samples..... 30

Figure 16. Sintered silicon nitride samples. 31

Figure 17. Green parts (after bulk drying) fabricated by CODE process. 32

LIST OF TABLES

PAPER I Page

Table 1. List of materials used in the experiments. 7

Table 2. Composition of paste used for binder content approximation. 10

Table 3. Silicon nitride formulation used for CODE process 11

Table 4. Printing parameters for silicon nitride formulation 13

Table 5. Density of silicon nitride parts with varying yttrium oxide + aluminum oxide additive concentration when sintered at 1830°C for 2.5 hours. 23

Table 6. Comparison of properties found in silicon nitride additive manufacturing process..... 33

NOMENCLATURE

Symbol	Description
β	Phase in silicon nitride with a tetragonal crystal structure
α	Phase in silicon nitride with a hexagonal crystal structure
η	Viscosity in Pa.s
Θ	Angle of rotation in XRD analysis
G’	Elastic shear modulus
G”	Viscous shear modulus
HIP	Hot Isostatic Pressing
CODE	Ceramic On Demand Extrusion

1. INTRODUCTION

This research investigates using the ceramic on-demand extrusion (CODE) process to fabricate complex 3D parts made of ceramics and ceramic composites, with applications to aerospace, energy, and biomedical industries. CODE is a patented freeform extrusion fabrication process developed at Missouri S&T. In the past, the parts that were fabricated using this process included aerospace structural components with high-temperature and ultra-high-temperature materials (e.g., alumina, zirconium diboride, and partially stabilized zirconia, silicon nitride, tungsten, molybdenum, and nickel). In the recent past the research focused on fabricating composite structures made of two or more materials that can be distinct materials or graded in compositions continuously as programmed to created parts with functionally graded materials. The current research focuses on fabricating parts based on non-oxide ceramics materials and refractory metals for ultra-high temperature and extreme temperature applications. The current research tasks include. (1) Fabricating non-oxide ceramics-based parts of near theoretical density with superior mechanical and thermal properties with consistency in part quality, (2) Development of silicon nitride paste formulations for producing high quality parts with consistency at an increased yield rate. (4) Evaluating the mechanical properties of specimens fabricated using non-oxide ceramics and refractory metals. (5) Development of novel support structure paste formulations for fabricating complex parts with minimum contamination and maximum quality.

PAPER

I. FABRICATION OF HIGHLY DENSE SILICON NITRIDE PARTS BY CERAMIC ON-DEMAND EXTRUSION PROCESS AND PRESSURELESS SINTERING

Sachin Choudhary[1], Austin Martin[2], Ming C. Leu[1], Greg Hilmas[2], Jeremy Watts[2], and Tieshu Huang[3]

[1]Department of Mechanical and Aerospace Engineering, Missouri University of Science and Technology, Rolla, MO 65409

[2]Department of Material Science and Engineering, Missouri University of Science and Technology, Rolla, MO 65409

[2]DOE National Security Campus, Honeywell FM&T
Kansas City, MO 64147

HONEYWELL FEDERAL MANUFACTURING & TECHNOLOGIES, LLC OPERATES THE KANSAS CITY NATIONAL SECURITY CAMPUS FOR THE UNITED STATES DEPARTMENT OF ENERGY / NATIONAL NUCLEAR SECURITY ADMINISTRATION UNDER CONTRACT NUMBER DE-NA0002839

ABSTRACT

Ceramic On-Demand Extrusion (CODE) is a patented additive manufacturing technology for manufacturing highly dense ceramic parts (99%) with reliable mechanical properties. In this study, silicon nitride parts with 15 wt.% additives (11.25 wt.% yttrium oxide & 3.75 wt.% aluminum oxide) were fabricated using the CODE process. Following the drying, a densification study and thermogravimetric analysis, to determine suitable sintering conditions, were conducted, specimens were sintered in a flowing nitrogen environment at atmospheric pressure. The sintered microstructure was analyzed, and grain size analysis was performed using scanning electron microscopy. Rheological tuning and characterization helped achieve rheology comparable to the polylactic acid (PLA) melts

used in fused deposition modeling process with the shear-thinning property. Density, hardness, and toughness measurements showed the achievement of comparable properties in silicon nitride specimens produced by the CODE process.

1. INTRODUCTION

Conventional forming processes to produce ceramic components use ceramic powders and/or ceramic slurries for part forming. Ceramic powders are used for die compacting and isostatic pressing. Ceramic slurries are typically used for slip casting or tape casting. Extrusion, injection molding techniques are used to form ceramic parts using fine ceramic powders in a polymer binder-loaded medium. Among those methods, some are limited to simple geometries, and some have a certain ability to fabricate complex shapes. Die compaction uses ceramic powder for forming small 2.5D parts (~117 mm diameter Parts using 500-ton capacity press [34]). Isostatic pressing is used for forming larger parts (1500 mm (diameter) and 2700 mm (height) with a 15-ton capacity press [35]) with high geometrical complexity in 3D. Slip casting is used for forming geometrically complex shapes using low viscosity slurries (55-70 mPa.s at 175 s^{-1}). In the injection molding process, geometrically complex shapes are fabricated, but it comes with recurring tooling costs (average cost of a single cavity mold ~12000$ and a very large and multi-cavity mold costs around ~80000$) and part design restrictions. The additive manufacturing method comes with the capability of fabricating any complex geometry possible without any extra tooling cost. ISO/ASTM 52900.2015 [1] has defined 7 categories of additive manufacturing, i.e., material extrusion, sheet lamination, binder jetting, powder bed fusion, material jetting, direct energy deposition, and vat

photopolymerization. The most widely used categories for ceramics are binder jetting, material extrusion, and vat polymerization. While binder jetting and vat polymerization come with the advantages of superior dimensional accuracy of ±10 microns, binder jetting fails to achieve densities yielding desirable structural/mechanical properties. In the parts fabricated by the vat photopolymerization process, the de-binding of polymers from the thick/big parts becomes challenging. The material extrusion-based processes have demonstrated the capability to achieve near theoretical density and the flexibility to accommodate fabrication of complex geometries (flexible to accommodate any dimensional complexity (2D, 2.5D, or 3D) and geometrical complexity (lines, surfaces, and solids)), as it has evolved to adapt formulations of high solid loading (50-55 vol%) over time with a lower binder content (1-3 wt. %) compared to other processes involving binder in the feedstock.

The patented technology of Ceramic On-Demand Extrusion (CODE) has demonstrated the capability of manufacturing near theoretical density ceramic parts after firing. In this process, high solid-loading (52 vol%) paste filaments are deposited layer-wise onto a substrate at room temperature. Infrared radiation was used for stiffening the layers due to drying, while also being surrounded by mineral oil, to solidify the surface of the current layer by drying but prevent crack formation due to excessive drying in previously printed layers [2][3]. The optimum amount of drying helps achieve accurate cross-sections without causing delamination. The progressive cavity pump-based extruding mechanism provides repeatability and precision in the printing process due to the positive displacement mechanism extruding a controlled amount of paste per unit time. In the past, the CODE process was successfully implemented to fabricate high-density

monolithic ceramic parts made of zirconia [3] and aluminum oxide [4]. Past research also showed superior mechanical properties for CODE processed ceramic parts [24].

In the presented study, the CODE process has been used for the fabrication of silicon nitride parts with the help of a pressureless sintering method for densification. The purpose of this study was two-fold. (i) to develop formulation and printing parameters for fabricating warp-free and delamination-free silicon nitride parts; and ii) to achieve high densities with a pressureless sintering method for establishing a cost-effective route for fabricating silicon nitride parts with mechanical properties comparable to traditional processing methods achieved by pressureless sintering.

Sintered silicon nitride ceramics have several unique properties, thus make them useful for a wide range of applications, including low density (3.17-3.23 g/cm^3), high thermal shock resistance, and strength retention at elevated temperatures (up to ~875°C [36]) make it suitable for aerospace and space applications [29]. The pressureless sintered silicon nitride offers comparable mechanical properties among other categories of silicon nitride ceramics with the least cost involved in comparison to all other methods [30]. Thus, sintered has found applications in reciprocating engine components, molten metal handling, bearings, and turbochargers [29]. Further, new applications for silicon nitride are still being discovered [5].

Sinterable silicon nitride powder formulations, such as 80-90% Si_3N_4, 6-12% Y_2O_3, and 2-8% Al_2O_3) have been shown to achieve high densities (≥98%) and high flexural strength (690 MPa at room temperature) among all other additives used in pressureless sintering of silicon nitride [6]. Previous AM research in silicon nitride helped highlight the challenges and potential research directions. Zhao et al. [7] were able to fabricate silicon

nitride parts using the robocasting method; the density achieved was near theoretical value, but the densification was achieved using pressure-assisted hot isostatic pressing (HIP). Geometrical accuracy and complexity of AM parts were also not discussed in their work.

Ventura et al. [8] were able to fabricate high-density silicon nitride parts using a vat photopolymerization method. Though the mechanical properties and densities achieved were comparable to those achieved by traditional methods, the HIP process incurs extra cost compared to the pressureless sintering method. The study of previous work overall indicated a need for a cheaper sintering route and need for better formulation for producing warp-free and delamination-free parts with comparable mechanical properties and better dimensional accuracy.

In this study, paste formulation with rheology comparable to polylactic acid (PLA) melts used in fused deposition modeling was developed for achieving dimensional accuracy comparable to parts fabricated by the Fused deposition modeling process (FDM). The formulation was optimized to achieve near theoretical density by minimizing organic contents as follows. (i) the most effective dispersants (while comparing four popular dispersants feasible for dispersing silicon nitride in aqueous medium) were chosen to achieve effective dispersion; and (ii) the binder content was optimized to achieve suitable yield strength in the printed layers. Printing parameters to achieve dimensional consistency and the highest green densities (56-61% TD) were established via first principles and experiments. Debinding and sintering temperature profiles yielding ~99% final part density were established. As a result, silicon parts fabricated with high dimensional accuracy and ~99% average density, demonstrating mechanical properties comparable to conventionally fabricated parts, were achieved. To demonstrate the usefulness of the process,

geometrically complex 3D parts, with and without the use of support material, were fabricated without warping or delamination.

2. EXPERIMENTAL PROCEDURE

2.1. STARTING POWDERS AND ORGANIC CONSTITUENTS

A commercial α-Si3N4 powder (M-11, HC. Stark, Germany) was used in this study. The mean particle diameter and the BET specific surface area were 0.60 μm and 12-15 m^2/g, respectively. The dispersants and binder used in the study along with the base used for pH adjustment of the formulation are listed in Table 1.

Table 1. List of materials used in the experiments.

Designation	**Company**	**Grade**
Silicon Nitride	H.C. Stark	M-11
Aluminum Oxide	Sumitomo Chemical Company	APK-50
Yttrium Oxide	H.C. Stark	Grade C
Disperbyk	BYK Additives	191
ZetaSperse	Air Products	Z-170
ZetaSperse	Air Products	Z-179
Darvan 821A	Vanderbilt Minerals	--
Methocel	Dow Chemical	J12MS
Potassium Hydroxide	Fisher Scientific	--

A mixture of 11.75 wt.% yttrium oxide (Grade C, HC. Stark, Germany, 99.95%) with a mean particle diameter of 0.90 μm and the BET specific surface 10-16 m^2/g and, 3.75 wt.% aluminum oxide (APK-50, High Purity Aluminum oxide (HPA), Sumitomo Chemical Company, Japan, 99.99%) was used as the sintering aid.

2.2. ZETA POTENTIAL ANALYSIS

The isoelectric point (IEP) is the pH at which the particle or molecules in consideration carries no net electrical charge. If the pH at the isoelectric point happens to be below 7, that indicates a high concentration of hydrogen ions (H^+) was required to neutralize the charge on particles/molecules. A low pH<7 thus indicates a presence of net negative charge and a pH>7 indicates the presence of net positive charge. This information helps one to determine the type of dispersant to be used for dispersing particles in consideration. A comparison of zeta-potential profiles of four potential dispersants was made to determine which dispersant induced maximum zeta-potential in the silicon nitride suspension. The comparison helps to identify the pH level which imparts the lowest viscosity in the suspension, alternatively the highest suspension stabilization. The comparison also helps to minimize the organic content in the paste by identifying the most effective dispersant. A 0.3 vol% dispersion (1 wt.% Darvan 821A) of silicon nitride powder (8 wt.% additives (3.1 Yttrium Oxide-Aluminum oxide)) was analyzed for the isoelectric point of starting powder mix. Aqueous suspensions of 10 vol% silicon nitride powder mix and 0.5 wt.%, 1 wt.%, and 2 wt.% of each dispersant (Dispersbyk-191, Zetasperse-170, Zetasperse-179, and Darvan 821A) were added to polyethylene jars, 20 ml each, and ball milled for 24 hours using aluminum oxide media at low speeds for deagglomeration. Zeta potential values were measured for different pH levels with the help of the Zetasizer Nano ZS90 machine (Malvern Instruments, Malvern, UK). A 0.001 M KCL buffer solution in deionized water was used in the test.

2.3. SINTERING AID CONTENT AND DENSIFICATION

The slurries were ball milled using aluminum oxide media at low ball milling speeds (10-15 rpm). The formulation while ball milling was of 40 vol% solids loading with 3 wt.% Darvan 821A. The paste formulation (as described in Table 3) was achieved from the ball-milled slurry by stepwise addition of methocel J12MS as the binder by mixing the same in the planetary mixer (ARE-310, Thinky USA Inc, CA, USA). CODE fabrication of the rectangular sample was achieved based on printing parameters described in Table 4. A densification study with different additive contents in the silicon nitride powder mix was conducted. Silicon nitride green samples with 10%, 15%, and 20% additive content (3.2 ratio of yttrium oxide & aluminum oxide) and 15% additive content (3.1 ratio of yttrium oxide & aluminum oxide) were sintered using a 3-inch Graphite sintering furnace. Binder burnout was performed at 400ºC for 2 hours. The samples were heated at a ramp rate of 10ºC to 1830ºC for a hold time of 2.5 hours. A subsequent natural cooling to room temperature was applied. The densities of the sintered sample were characterized using the Archimedes principle [21].

2.4. BINDER CONTENT

The initial silicon nitride suspension formulation is given in Table 2. The resulting suspension was ball milled for 24 hours in deionized water using aluminum oxide milling media. Following ball milling, Methocel J12MS was added, and the paste was mixed in a planetary mixer (ARE-310, Thinky USA Inc, CA, USA) at 2000 rpm for a total of 20 minutes in steps of 2 minutes each with an intermittent cooling time of 5 minutes. Pastes containing 0 wt.%, 0.5 wt.%, 1.5 wt.% of Methocel were rheologically characterized with

increasing shear rate using a Malvern Kinexus rheometer (Ultra$^{+,}$ Malvern Instruments Ltd, Worcestershire, UK) for measuring yield stress of paste while approaching the shear rate of ~0.1 s^{-1} from high shear rate value of 100 s^{-1}.

Table 2. Composition of paste used for binder content approximation.

Components	Weight (g)	Density (g/cc)	Volume (cc)	vol %
85 % Silicon nitride (abcr -M11), 11.25% Yttrium oxide, 3.75% Aluminum oxide))	145.3	3.3	44.0	45
Deionized water	51.5	1.0	51.5	53
Dispersant (Darvan 821A)	2.9	1.3	2.2	2

2.5. PREPARATION OF PASTE FOR CODE PROCESS

Based on results from binder content determination experiments, a binder content of 0.8 – 1.0 wt. % was found to impart enough yield strength to the paste for fabricating green parts capable of retaining shape during the fabrication process. The silicon nitride formulation with 0.8-1 wt.% binder was mixed in a planetary mixer (ARE-310, Thinky USA Inc, CA, USA) at 2000 rpm for a total of 20 minutes in steps of 2 minutes each with intermittent drying of moisture at 90°F to reach a solid loading of 50-52 vol%. Table 3 shows the formulation finalized after dispersant content and deionized water were adjusted to achieve polylactic acid (PLA) melt-like rheology which is used in fused deposition modeling based additive manufacturing methods.

Table 3. Silicon nitride formulation used for CODE process

Components	Weight (g)	Density (g/cc)	Volume (cc)	Volume (%)
85 % Silicon nitride, 11.25 % Yttrium oxide, 3.75 % Aluminum oxide	145.3	3.3	44.3	52.5
Deionized water	28.2	1.0	28.2	33.4
Dispersant (Darvan 821A)	12.2	1.3	9.8	11.6
Binder (Methocel - J12MS)	1.5	0.7	2.1	2.5

2.6. RHEOLOGICAL CHARACTERIZATION

Rheological characterization of the paste formulation (Table 3) was conducted using the Malvern Kinexus rheometer (Ultra^{+}, Malvern Instruments Ltd, Worcestershire, UK) for viscosity profiles and shear moduli profiles after adjusting the formulation to achieve comparable rheology to PLA filament melts which are used in a fused deposition-based 3D printing method. Rheological characterization of the paste formulation (Table 3) was carried out using the Malvern Kinexus rheometer (Ultra^{+}, Malvern Instruments Ltd, Worcestershire, UK) for viscosity profiles and shear moduli profiles after adjusting the formulation to achieve comparable rheology to PLA filament melts which are used in fused deposition-based 3D printing method. A parallel plate setup with a 0.75 mm gap was used for the measurements. The sample volume used in the tests was 0.4 ml. The tests were conducted with a solvent trap for avoiding the drying of the paste. Before each rheological test, the homogeneity/consistency of the paste was ensured by running a constant shear rate (20 s^{-1}) test on the paste until a stable viscosity was achieved in the paste sample.

Before each rheological test, the homogeneity/consistency of the paste was ensured by running a constant shear rate (20 s^{-1}) test on the paste until a stable viscosity was achieved in the paste sample.

2.7. THERMOGRAVIMETRIC ANALYSIS (TGA)

Thermogravimetric analysis (TGA) was performed on the paste formulation (Table 3) to determine the temperatures at which ramp rates and hold times may be critical during the binder removal process. A mass of 10 mg was heated in air at 5°C/min to 600°C using a thermal analysis instrument (STA 409C; Netsch, Selb, Germany). The mass loss profile was analyzed to determine the binder burnout temperature profile.

2.8. PART FABRICATION BY CODE PROCESS

Figure 1 shows the ceramic on-demand extrusion (CODE) machine setup used in the fabrication of samples for the presented study.

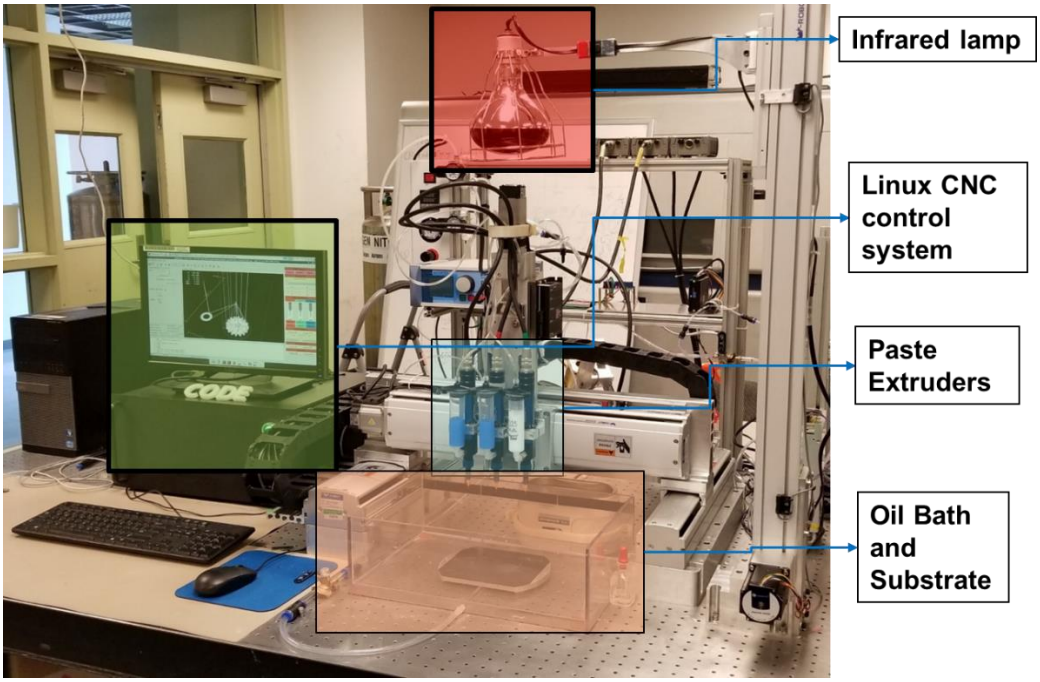

Figure 1. Setup for the Ceramic On-Demand Extrusion process

The CODE process consists of the following steps. (1) extrusion & tool-path traversing (aqueous paste extruded using a high precision auger with a tool head traversing at a designated speed), (2) oil bath (light mineral oil) with liquid level control to surround the part, but only up to just below the top surface, and prevent warping by eliminating drying from the sides of the part, (3) drying the top layer using infrared radiation to make the surface layer stiff enough to support subsequently deposited layers, and (4) repeat of the above steps.

Silicon nitride (Si_3N_4) billets were fabricated using CODE with the formulation in Table 3 and the printing parameters in Table 4.

Table 4. Printing parameters for silicon nitride formulation

Printing Parameters	Values
Infill speed	310 mm/min
Perimeter speed	300 mm/min
Extrusion speed	317 mm/min
Coasting distance	5 mm
Extrusion width	0.4 mm
Layer thickness	0.45 mm
Nozzle Diameter	0.68 mm

To finalize the process parameters for the CODE process, the following factors were critically determined to fabricate layers accurately and precisely. (i) extrusion width, (ii) extrusion rate, (iii) nozzle traverse speed, and (iv) layer height. Green parts were fabricated using the extrusion spacing/width concept depicted in Figure 2, which highlights an equation for raster spacing in gapless printing without overflow. The average extrusion width was calculated using ImageJ software (National Institutes of Health, Bethesda, MD)

by measuring the extrusion width of extruded filament at multiple locations from the high-resolution photographs of filaments deposited in a serpentine fashion. The average extrusion width was 906 microns using a nozzle diameter of 680 microns, a layer height of 500 microns, and a nozzle traverse speed of 438 mm/min. The raster spacing was thus calculated based on calculated average extrusion width and layer height based on Figure 2.

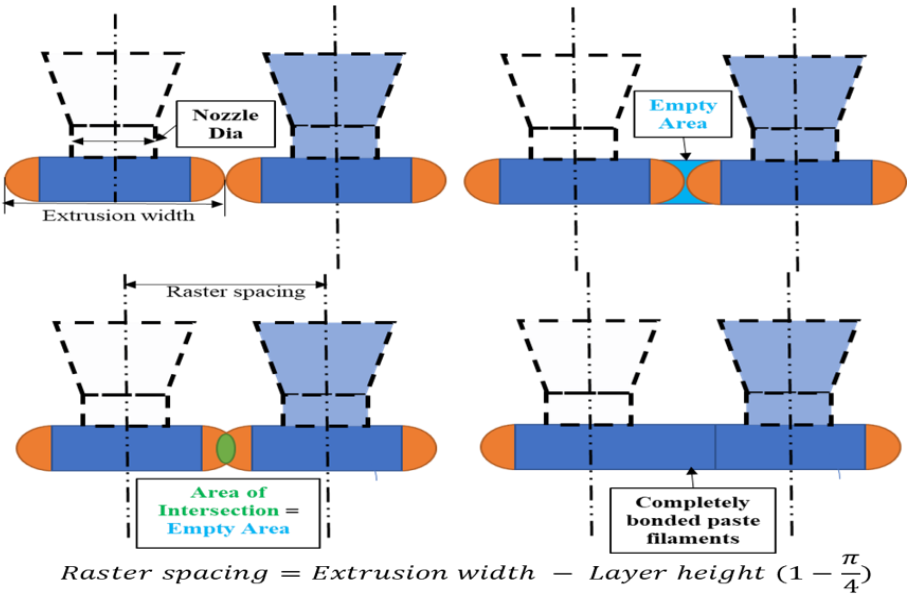

Figure 2. Raster spacing concept depiction

2.9. DENSIFICATION STUDY PROCEDURE

Three specimens were sintered in each run. All samples were held for 2.5 hours at the indicated sintering temperature. A powder bed was used to surround the samples, its composition was 75% silicon nitride as received powder and 25% boron nitride powder which was ball milled for 36 hours at 30-45 rpm.

2.10. HARDNESS & FRACTURE TOUGHNESS MEASUREMENT

The sintered samples were ground with a 120-grit diamond grinding wheel (Tech diamond tools, California, USA). Thereafter, the samples were polished to a 0.25-micron surface finish using progressively finer diamond abrasives using an automated polishing machine (Struers Inc, Tegramin-30, Cleveland, Ohio). The hardness measurements were performed using a Vickers hardness testing machine (Duramin-5, struers Inc, Cleveland, Ohio), which automatically calculates the vertical and horizontal intercepts. The fracture toughness measurements were determined using a micro indentation hardness tester (LM110 series, LECO, MI, USA) with a load of 30kg. The dimensions of the indent and the extending cracks were captured using an optical microscope (RH-2000 system, Hirox USA Inc, New Jersey, USA).

3. RESULTS

3.1. CHARACTERIZATION OF POWDERS & SLURRIES

The isoelectric point (IEP) was determined by performing zeta potential measurements as a function of pH on a 0.3 wt.% suspension of silicon nitride (92 wt.%), yttrium oxide (6wt.%), and aluminum oxide (2 wt.%) in deionized water (1 wt.% Darvan 821A) (Figure 3). As shown in Figure 3, the zeta-potential was ~14 mV at a pH of 2, and then decreased steadily to ~-28 mV at a pH of 5. The zeta potential was zero at a pH of ~2.7 which was thus determined as the isoelectric point. A pH=2.7 indicates a highly acidic surface, which is not surprising since the Si_3N_4 powder would be expected to have SiO_2 on the surface of the powder [37], the anionic dispersants described earlier were selected for suspension stabilization.

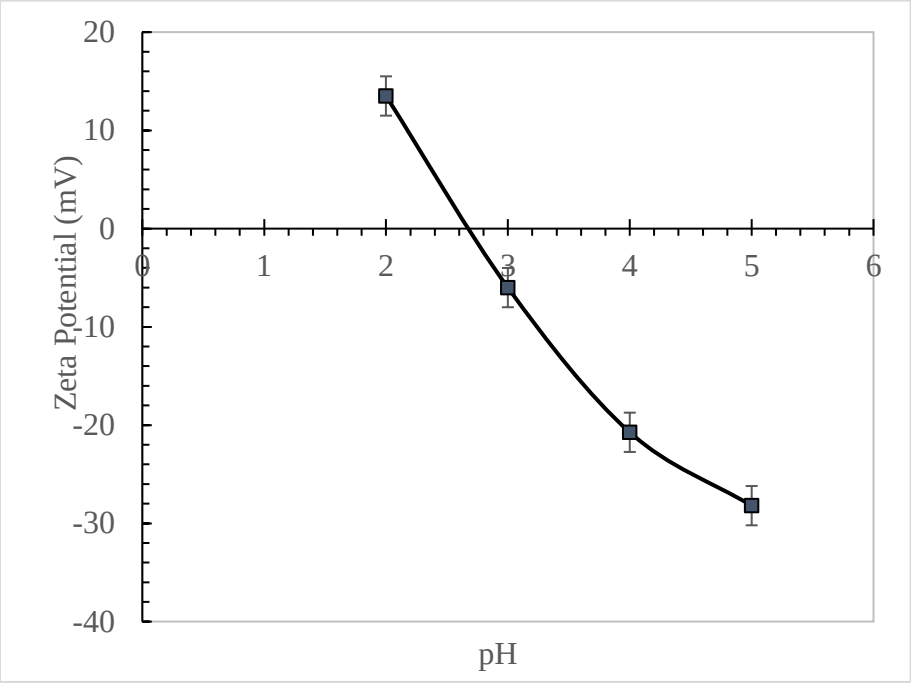

Figure 3. Zeta potential measurements for silicon nitride formulation powder mix.

Figure 4 shows the zeta potential profiles of four candidate dispersants in consideration. For 2 wt.% Dispersbyk-191 suspension, the zeta-potential was measured as 42 mV at pH = 4, and the zeta potential continued to decrease with an increase in pH to 11. A similar decreasing trend in zeta potential was observed in Zetasperse179(Z179) and Zetasperse170(Z170) based suspensions, with increasing pH values. At pH = 11, Darvan 821A had the maximum charge, thus the most effective dispersant was determined to be Darvan 821A which induced a maximum charge on the particles, thus maximizing the zeta potential values. Darvan 821A was also used by past researchers [14][31] in successfully fabricating silicon nitride parts using the robocasting method. Thus, Darvan 821A was used ih the formulations of silicon nitride paste in the presented study.

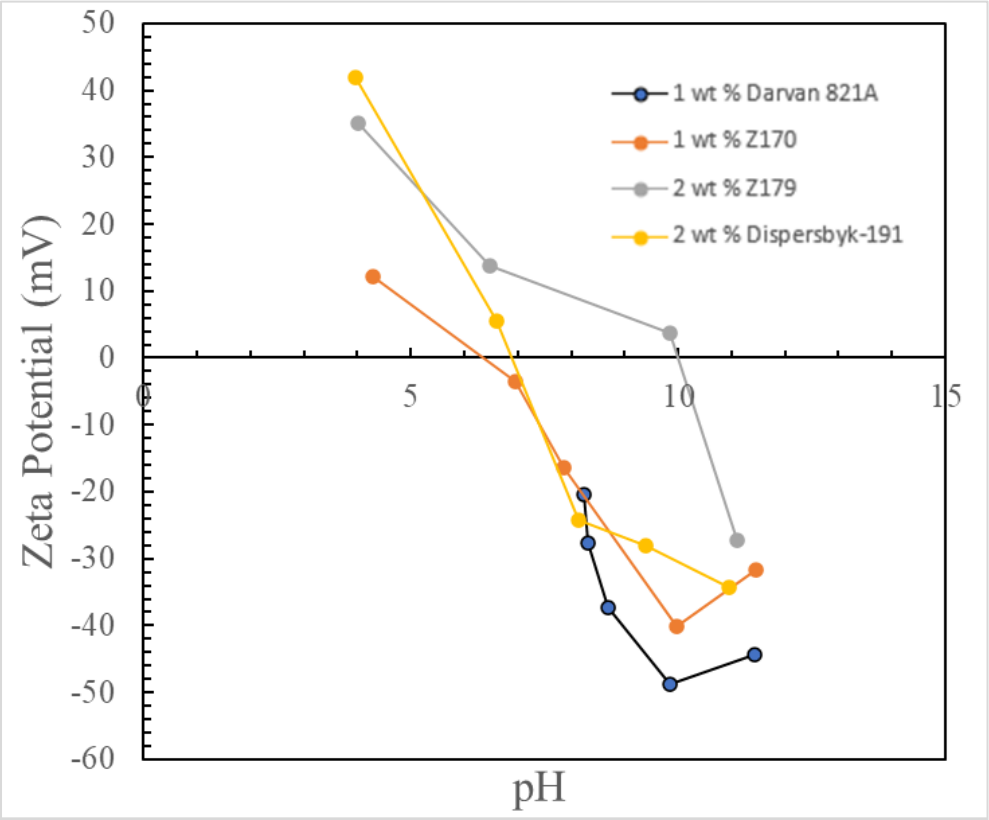

Figure 4. Zeta profile for different dispersants for silicon nitride.

3.2. RHEOLOGICAL CHARACTERIZATION

A certain degree of yield stress is desirable to prevent unwanted deformation after paste deposition. However, the maximum value of yield stress is limited by the fact that a shear-thinning formulation is needed to enable extrusion of the paste. Yield stress measurements were performed by varying the amount of binder content in the ball-milled silicon nitride paste formulation described earlier (Table 3) using 1 wt.% Darvan 821A. Figure 5 captures the variation in dynamic stress with an increase in shear rate, showing the dynamic stress vs shear rate profile for suspensions containing 0 wt. %, 0.5 wt.%, and 1.5 wt.% of binder content in the formulation. The increase of binder content caused an increase in yield stress of the formulation. The pastes with all three binder contents were

tested for printing. It was found that the yield stress for 0.5 wt.% binder content was it was too low, resulting in deformation after printing.

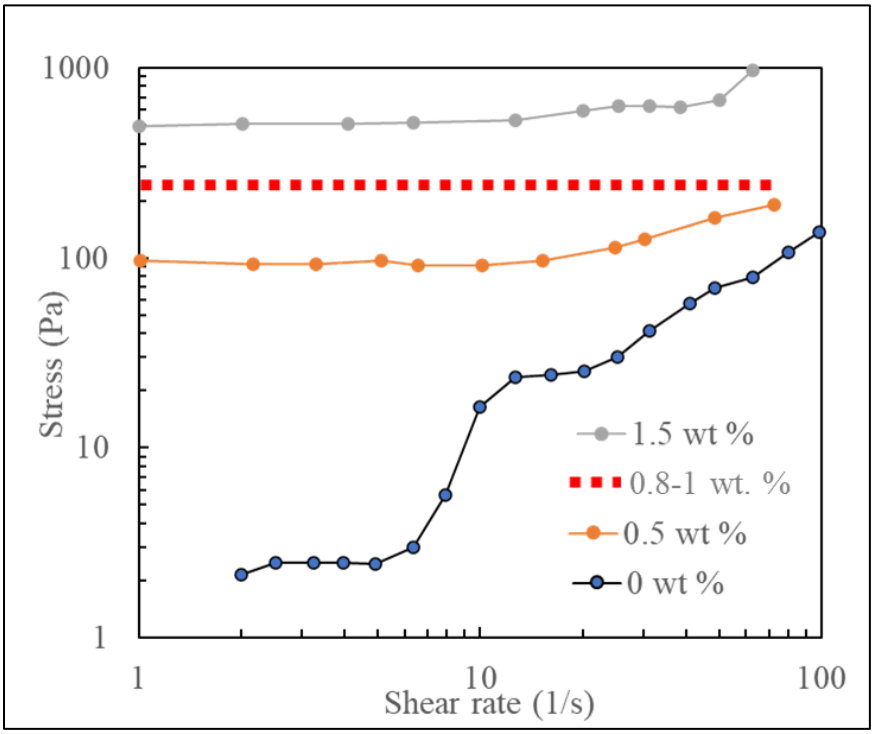

Figure 5. Variation of yield stress in silicon nitride-based CODE formulation with binder content.

The variation in viscosity of paste with increasing shear rate was captured for quantifying the viscosity and confirming a shear-thinning behavior in the paste. Figure 6 shows the viscosity profile of silicon nitride formulation (Table 3), with increasing shear rate, used in the CODE process, which is comparable to the polylactic acid (PLA) melt viscosity profiles presented by Kitoba et al. [11]. A viscosity of 4000 Pa.s was observed at 0.1 s^{-1} with a shear-thinning behavior for the silicon nitride formulation which is

comparable to the viscosity of the polylactic acid (PLA) melts used in fused deposition modeling based additive manufacturing processes.

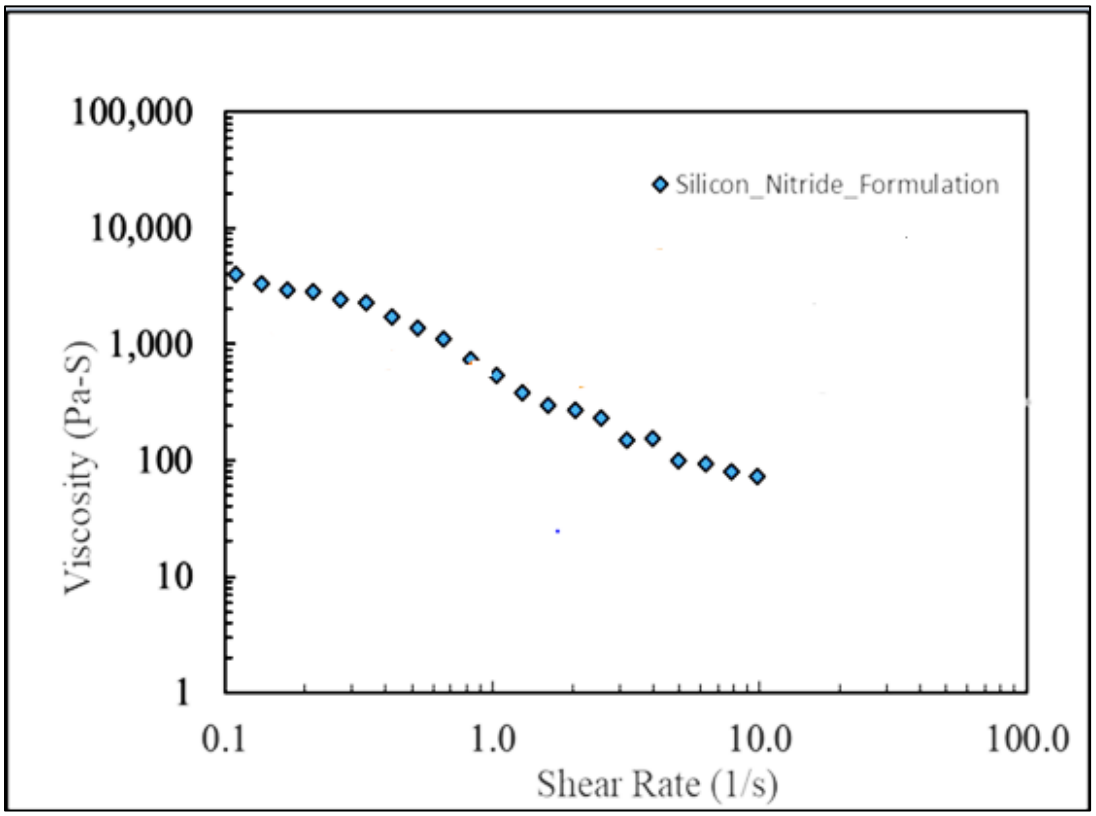

Figure 6. Viscosity profiles of silicon nitride formulation.

Figure 7 shows the elastic shear modulus (G') & viscous shear modulus (G") measurement profiles for amplitude sweep test with an increase in complex shear strain (%), for silicon nitride formulation (Table 3). An elastic shear modulus of ~200,000 Pa was measured at a complex shear strain amplitude of 0.01 %, which was found comparable to the polylactic acid (PLA) melts used in fused deposition modeling based additive manufacturing processes operating at a temperature of 180°C. [12]

The comparable rheology achieved helps in ensuring a formulation which will yield parts with consistent dimensions.

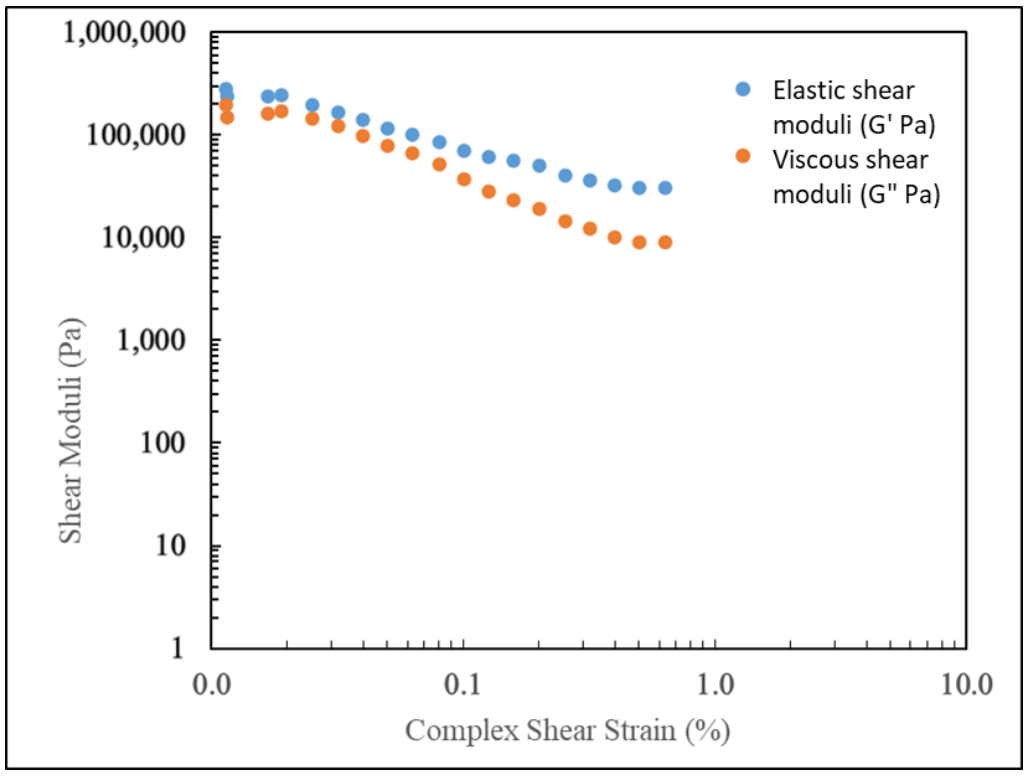

Figure 7. G' and G" for silicon nitride formulation (Table 4) at room temperature.

3.3. BINDER BURNOUT

To reduce defects and improve density and overall part quality, thermogravimetric analysis (TGA) was conducted to better understand the burnout process. Figure 8 shows the TGA curve for the silicon nitride formulation (Table 3). The first major change in the rate of weight loss came around 130°C. The decomposition temperature of DARVAN 821A is also found at around 130°C. The decomposition of methocel has been found to take place in the temperature range of 200°C - 380°C [38]. The two stages of major change

in weight loss occurred around 210°C and 360°C thus corresponding to the decomposition of methocel. Thus, the entire burnout process takes place in three stages, which are approximately. 130°C, 210°C, and 360°C. Thus, a three-stage binder burnout profile was adopted to minimize any binder burnout defects.

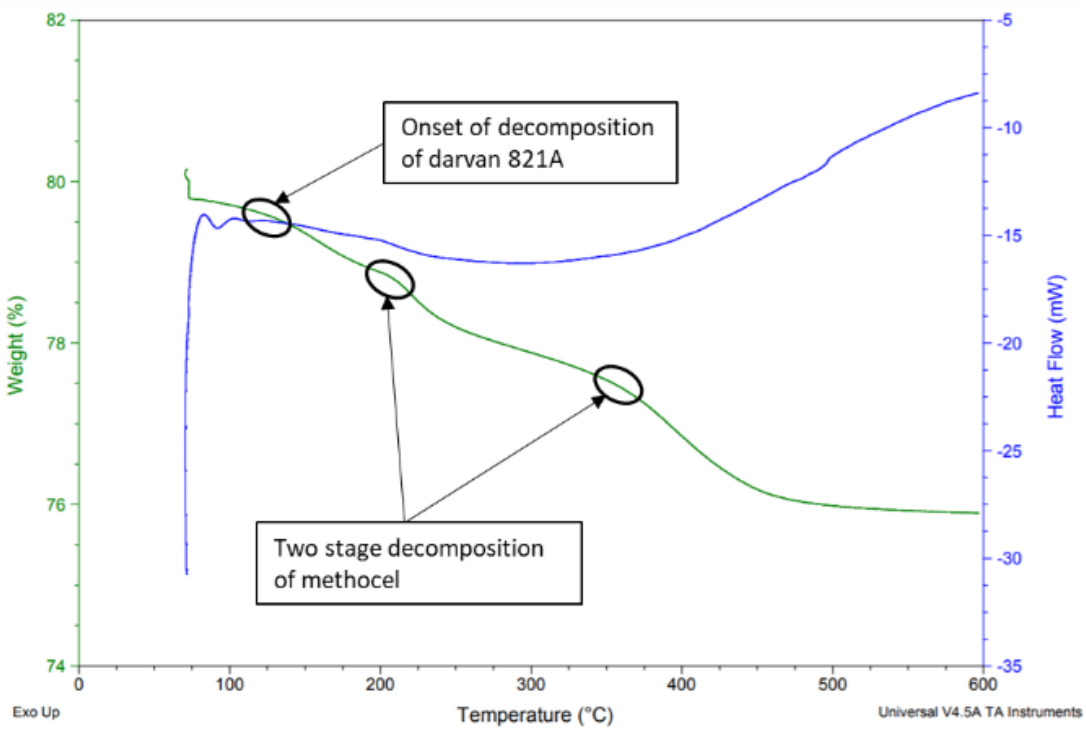

Figure 8. TGA curves for determining binder burnout cycle for the 50 vol% silicon nitride paste formulation.

The TGA-based weight loss curve was used to develop a binder burnout temperature profile for the green parts. Binder burnout was performed by heating the green parts in nitrogen at ~5°C/min to 130°C, with a hold of 1 hour, subsequently, it was heated ~5°C/min to 210°C for 1 hour and final at~5°C/min to 400°C for 2 hours in a burnout furnace (Dentsply International Inc, Vulcan 3-550 series, York, PA). After the de-binding,

the temperature was ramped at the rate of 15°C/min to the sintering temperature of 1830°C and held for 2.5 hours for densification in a 3-inch Graphite furnace. Figure 9 shows the sintering cycle followed in the pressureless sintering process.

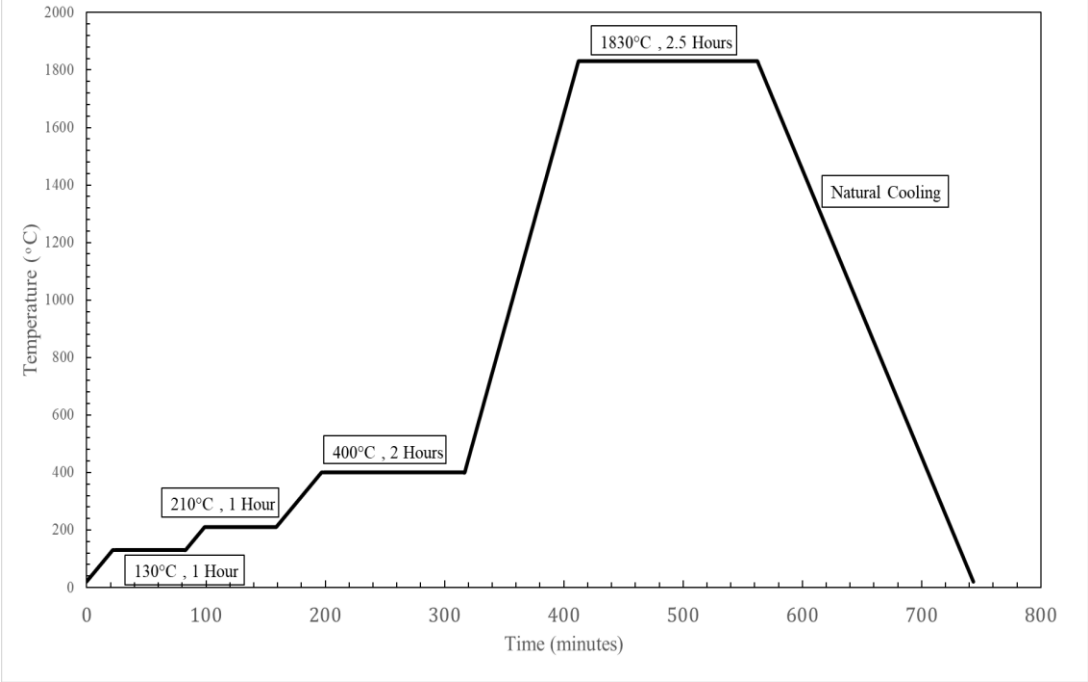

Figure 9. Sintering cycle for silicon nitride parts fabricated by CODE process in 0.1 MPa nitrogen gas environment.

3.4. ADDITIVE CONTENT AND SINTERING TEMPERATURE

Rectangular specimens were fabricated using the printing parameters outlined in Table 4. These billets were then sintered to different final sintering temperatures as per the experiment's requirement. The densification study with different levels of additive content (10%, 15%, and 20% of yttrium oxide and aluminum oxide in 3.2 ratio and, 15% of yttrium oxide and aluminum oxide in 3.1 ratio) was conducted by firing the CODE fabricated silicon nitride samples at 1830°C for a dwell time of 2.5 hours. An increasing trend in

densification was observed with increase in additive content in the powder mix with 3.2 ratio of yttrium oxide and aluminum oxide. The particle size distribution, production method of powders, and composition of powders greatly affect the densification trends [28]. A similar trend in increased densification with additive content was observed by Yang et al. [9], where an additive content of 14 wt.% (5.2 ratio of yttrium oxide and aluminum oxide) produced the highest density (~100% relative density) when sintered at temperatures of 1830°C. While 20% of yttrium oxide and aluminum oxide in a ratio of 3.2 produced parts with density ~96%, the 15%% of yttrium oxide and aluminum oxide in a ratio of 3.1 produced parts with density ~98%. Table 5 summarizes the sintered density achieved by using different additive contents in the formulation. When the ratio for yttrium oxide to aluminum oxide was changed to 3.1, the relative density increased to 98% for the sintered parts, thus the 3.1 ratio of additives at 15 wt. % of powder mix was used for the formulation.

Table 5. Density of silicon nitride parts with varying yttrium oxide + aluminum oxide additive concentration when sintered at 1830°C for 2.5 hours.

Additive Concentration (wt. %)	**Relative Density (%)**
10 (3.2)	92.0
15 (3.2)	95.5
20 (3.2)	96.0
15 (3.1)	98.0

Figure 10 shows the average densities achieved for the nozzle traverse speed of 310 mm/min and sintered at different temperatures (1800°C, 1820°C, and 1830°C) for 3 specimens in each run. All samples were held for 2.5 hours at the indicated sintering

temperature. The plot in blue corresponds to a travel speed of 310 mm/min. For a sample of 3 rectangular billets for each run, for the firing temperature of 1800°C, an average density of 92.4 ± 0.2% was observed, for the firing temperature of 1820°C, an average density of 94.0 ± 0.4% was observed, for the firing temperature of 1830°C, an average density of 98.6 ± 0.7%, all the density measurements were conducted according to ASTM C373 [21].

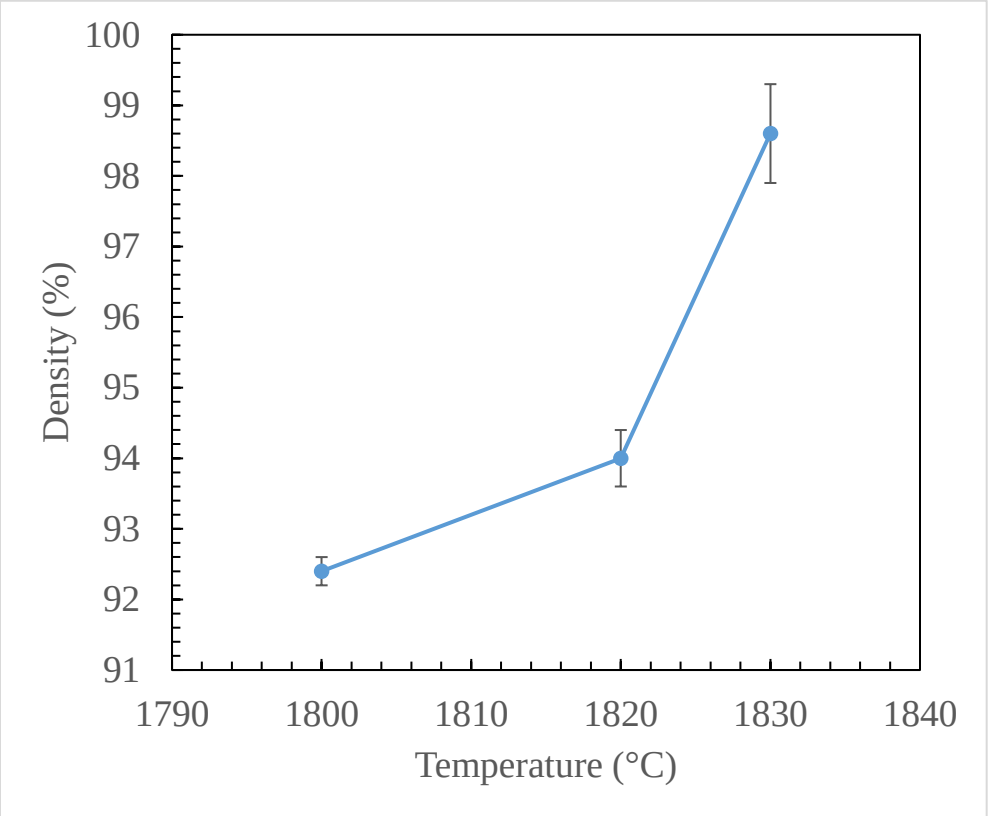

Figure 10. Densities in silicon nitride specimens at a nozzle travel speed of 310 mm/min

3.5. FABRICATION AND FIRING FOR DENSITY CHARACTERIZATION

The fabrication of the 10 samples of rectangular billets was performed using the paste formulation described in Table 3 and printing parameters enlisted in Table 4. The dimensions achieved in samples after sintering was 30mm x 30mm x 2.5mm. The picture in the bottom part of Figure shows some samples after sintering.

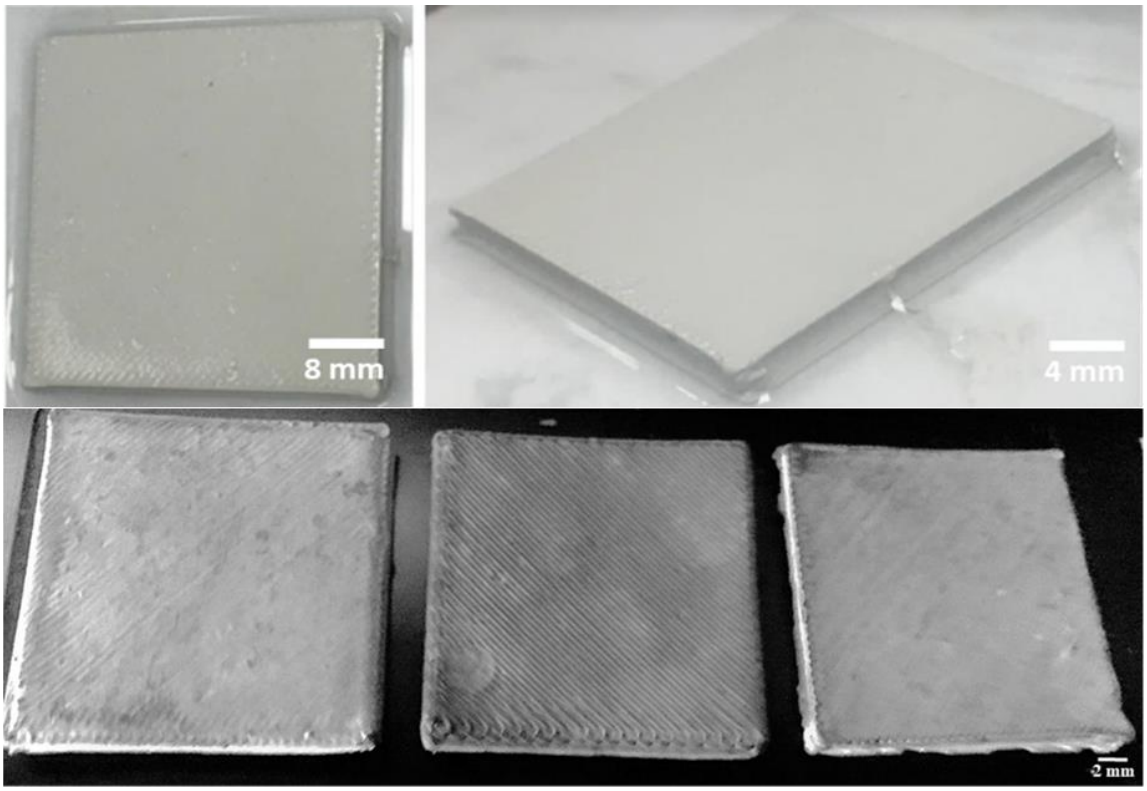

Figure 11. As-printed silicon nitride billets (above), sintered silicon nitride billets (below).

3.6. DENSITY CHARACTERIZATION

The density measurements of rectangular billets as measured by the Archimedes method showed an average density of 98.6 ± 0.7 % was achieved through the CODE process for a sample size of 10 billets in total. The sintering schedule was as indicated in

Figure 7. The dimensions achieved in samples after sintering was 30mm x 30mm x 2.5mm. The average density achieved in the CODE fabricated parts were found to be comparable to other additive manufacturing processes. Zhao et al. [14] achieved an average density of 98.6% in silicon nitride samples fabricated by the robocasting process and sintered by the hot isostatic pressing (HIP) method. Ventura et al. [17] were able to achieve an average density of 97.9 % for silicon nitride samples fabricated by Direct light printing (DLP) and sintered by the HIP method. Cappi et al. [18] were able to achieve an average density of 97% for silicon nitride samples fabricated by the direct inkjet printing method.

3.7. HARDNESS & FRACTURE TOUGHNESS

An average hardness value of HV0.3 ~ 1637 ± 116 kg/mm2 was calculated for a batch of 5 samples with 4 indents in each sample, a force of 2.98 N (0.3 kg) was used for hardness measurement. Samples were fabricated by formulation of Table 3 and sintered using the sintering schedule as described in Figure . Figure 13 shows the indentation in the sintered and polished sample for hardness testing as per ASTM C1327 [22], the average value of the horizontal and vertical diagonals of the indentation was found as 18.59 microns and 18.34 microns respectively. The hardness value observed in the CODE fabricated silicon nitride samples was found comparable to the hardness values achieved through other AM methods of fabricating silicon nitride parts. Whereas Liu et al. [16] were able to achieve 14.63 GPa of hardness value in silicon nitride samples fabricated by stereolithography (SLA) process and sintered using gas pressure sintering method, Ventura et al. [17] were able to achieve an average hardness value of 16.5 for silicon nitride samples fabricated by Direct light printing (DLP) and sintered by the HIP method. Furthermore,

Cappi et al. [18] were able to achieve an average hardness value of 17.0 GPa for silicon nitride samples fabricated by the direct inkjet printing method. It was observed that the hardness in present samples was comparable to samples densified by advanced densification methods of gas pressure sintering and hot isostatic process method.

Fracture toughness was calculated using the following formula for 6 specimens using the direct crack Vickers indentation method.

$$K_{IC} = \varphi * \left(\frac{E}{H}\right)^{\frac{1}{2}} * \frac{P}{c^{\frac{3}{2}}}$$

where.

Φ = 0.016; is a constant

E = 300 GPa (Young's modulus) [32]

H = 16.37 GPa (Hardness) (Average hardness value observed)

P = 294.3 N (load)

c = 237 μm (crack length)

Figure 12 shows the diamond indentation using a Vickers's indentation machine based on the method proposed by Anstis et al. [23]. Average fracture toughness of 5.5±0.49 MPa$\sqrt{m}$ was determined based on the calculations. Liu et al. [16] were able to achieve 5.8 ± 0.42 MPa$\sqrt{m}$ of fracture toughness value in silicon nitride samples fabricated by stereolithography (SLA) process and sintered using gas pressure sintering method. Ventura et al. [17] were able to achieve an average fracture toughness value of 4.5 MPa$\sqrt{m}$ for silicon nitride samples fabricated by Direct light printing (DLP) and sintered by HIP method, while Cappi et al. [18] were able to achieve an average fracture toughness value of 4.4 MPa$\sqrt{m}$ for silicon nitride samples fabricated by the direct inkjet printing method.

3.8. MICROSTRUCTURE OF FABRICATED SILICON NITRIDE PARTS

Figure 13 shows the microstructure of an unetched polished sample obtained from scanning electron microscopy. The microstructure exhibits little porosity which agrees well with the density measurements already discussed.

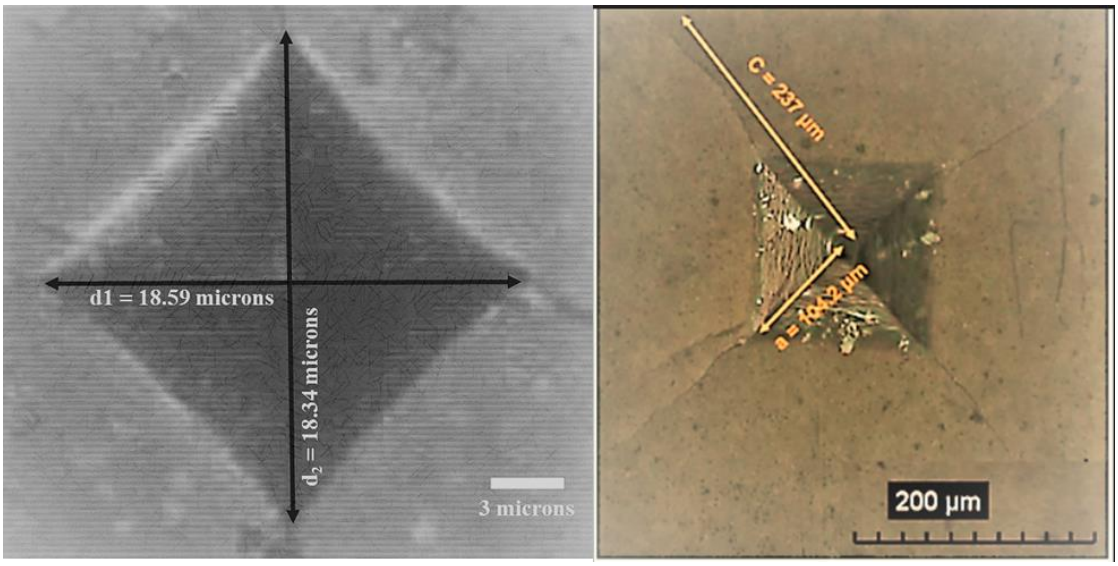

Figure 12. Hardness indentation in polished silicon nitride sample (left), Vickers's indentation for evaluating fracture toughness (right).

The dark grey phase is Si_3N_4 grains while the lighter phase surrounding the Si_3N_4 is yttrium aluminum garnet (YAG) produced from the aluminum oxide and yttrium oxide sintering aids. There appear to be many small (1-5 micron) grains with some large (10+ micron) grains interspersed. Grain size measurements based on measurements from 42 grains in total were performed by capturing planar intercepts using ImageJ software [25] showed an average grain size of 11.33 microns calculated according to the method described by Mendelson et al. [26].

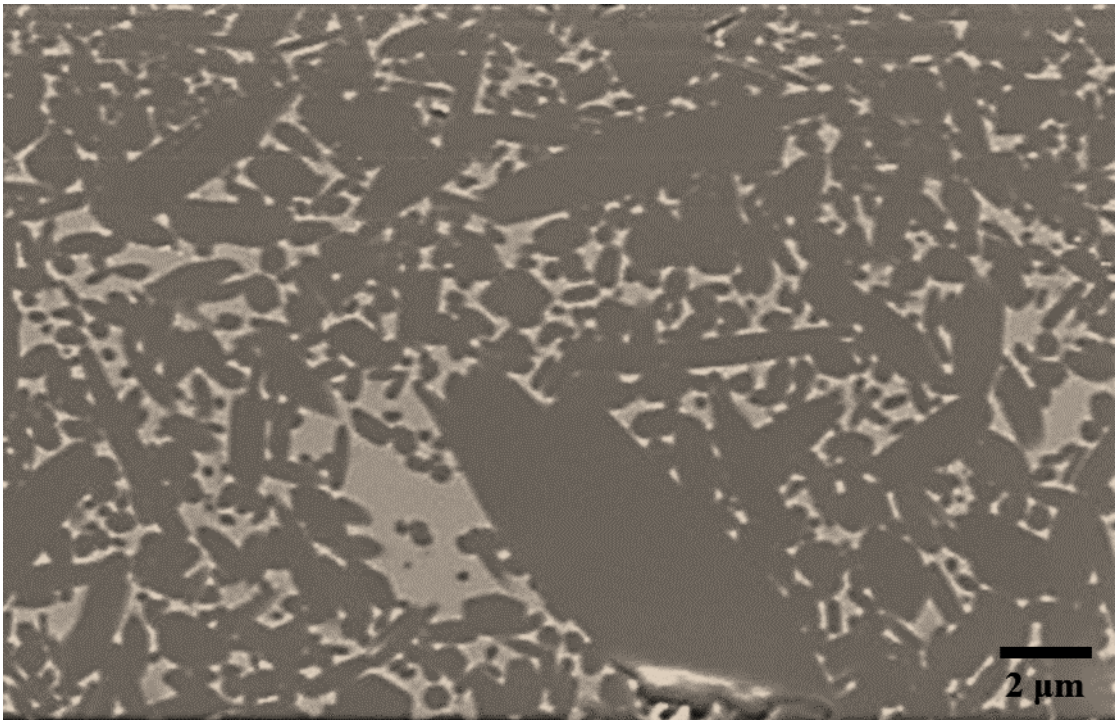

Figure 13. Microstructure for sintered silicon nitride samples.

3.9. XRD (X-RAY DIFFRACTION) ANALYSIS

The XRD analysis of sintered samples (Figure 15) shows the absence of the tetragonal (α) phase of silicon nitride and there is a 97-98 % presence of β-silicon nitride phase. The presence of the β phase confirms the liquid phase sintering phenomenon in the specimens, which is indispensable for achieving high strength silicon nitride material. The α to β phase transition during the liquid phase sintering of silicon nitride is a commonly identified phenomenon [13][33]. Figure 14 shows the XRD pattern of silicon nitride powder formulation mix, where only ~5-6% β-silicon nitride phase was observed initially while 79-80% of the silicon nitride was found in the α phase.

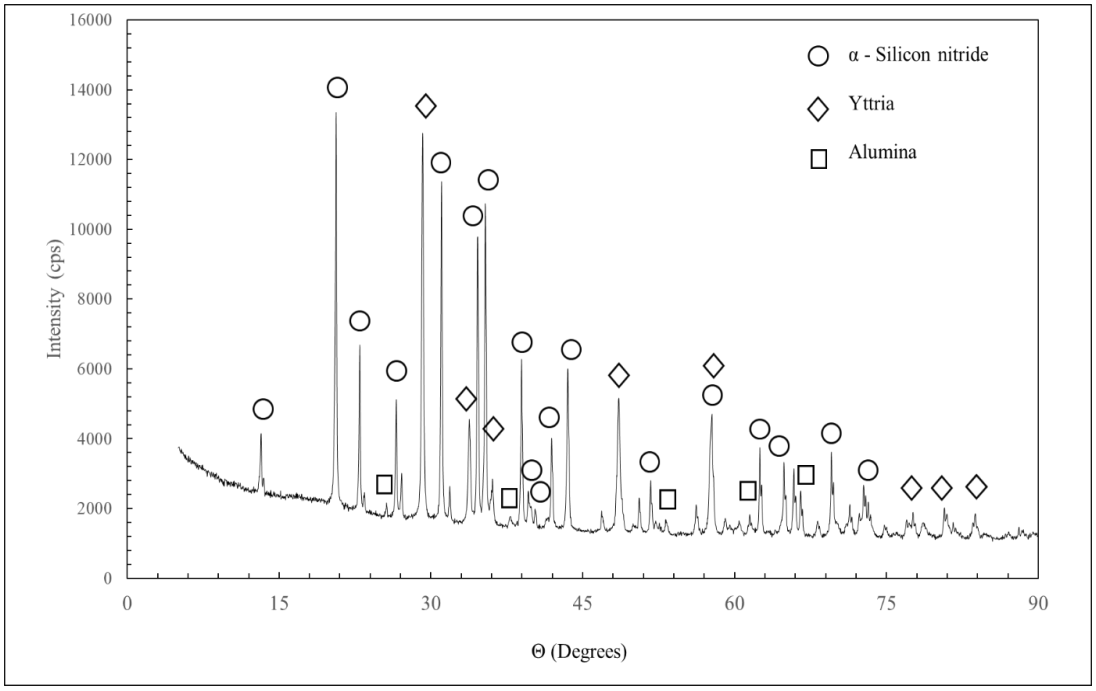

Figure 14. XRD (X-ray Diffraction) pattern analysis of silicon nitride powder mix.

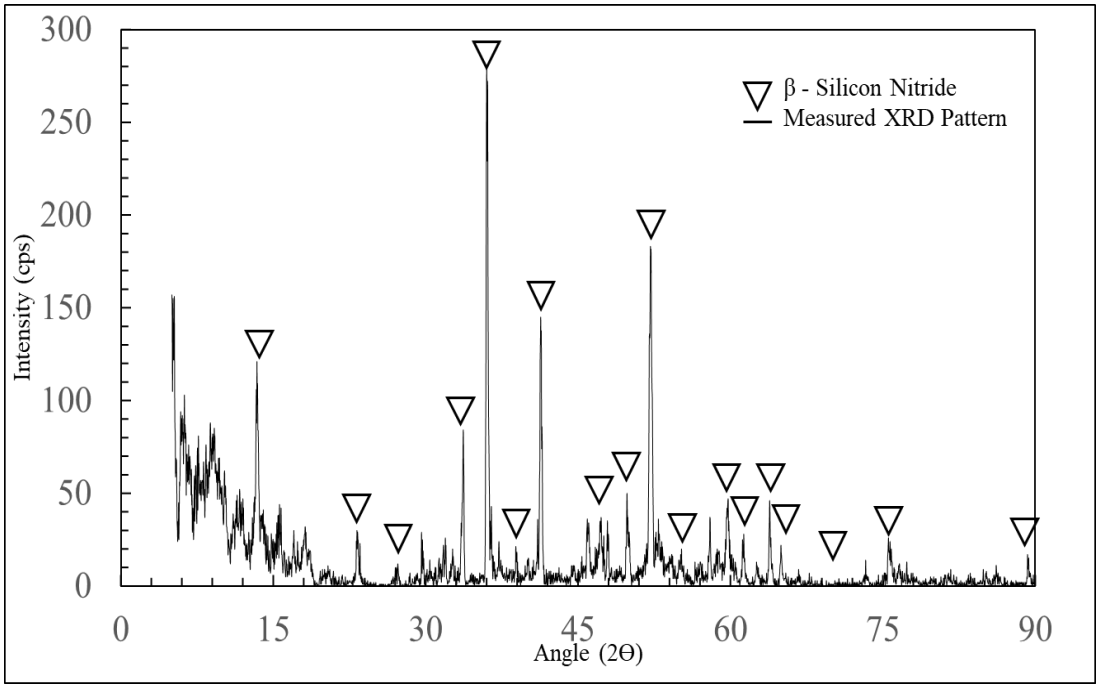

Figure 15. XRD pattern of sintered silicon nitride samples.

3.10. CODE FABRICATED SILICON NITRIDE PARTS

The process parameter tuning of the printing process helped achieve 3D fabricated parts with minimum to no flaws in them, while a few demonstration parts were successfully fabricated and fired for densification. Figure 16 on the left shows a sintered double-helical gear fabricated using a 680µm nozzle. The layer height for the fabrication process was 450µm and decreased to 380µm after firing. The compressor housing on the right was fabricated using an aqueous paste formulation with calcium carbonate (45 vol% with 2 wt.% Darvan 821A & 0.9 wt.% Methocel J12MS as a binder) as the sacrificial material for fabricating the support structure. Figure 17 presents several silicon nitride parts including gears, turbine impeller, and honeycomb fabricated by the CODE process with the formulation in Table 3 and process parameters in Table 4, then sintered at 1830℃ for 2.5 hours. All the sintered parts were crack-free as a highly consistent and homogeneous paste was used for fabricating the green parts.

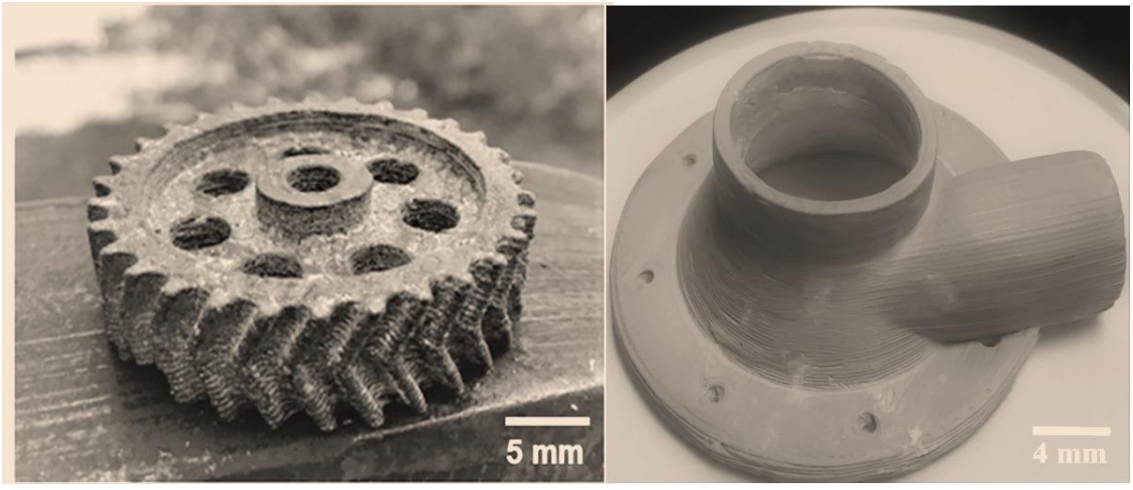

Figure 16. Sintered silicon nitride samples.

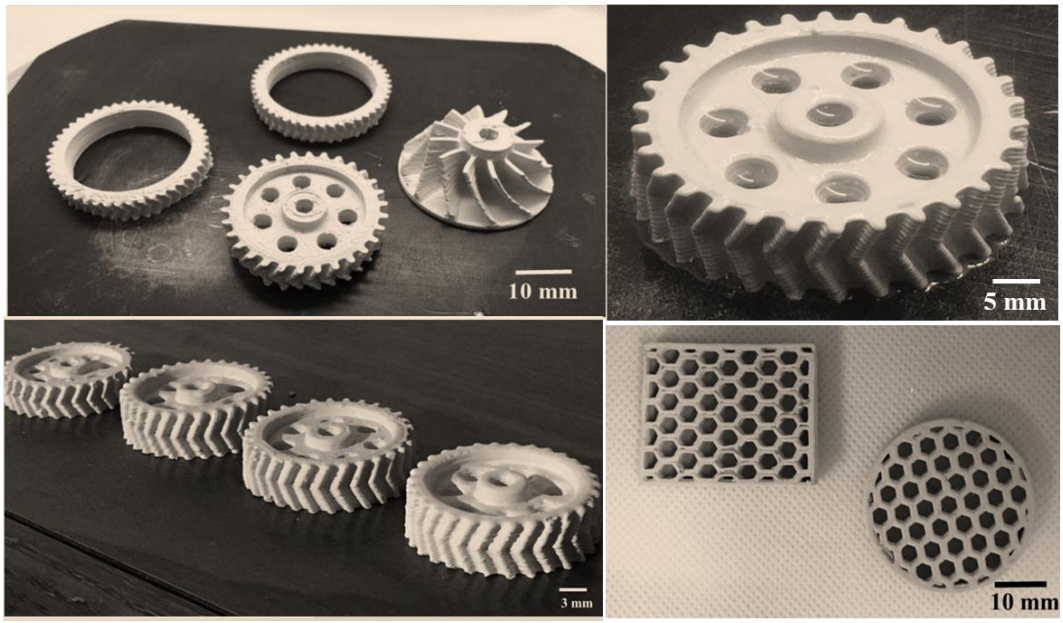

Figure 17. Green parts (after bulk drying) fabricated by CODE process.

3.11. COMPARISON WITH OTHER MANUFACTURING PROCESSES

The properties obtained in sintered silicon nitride parts were compared to the properties achieved by other methods of additive manufacturing of ceramics. Table 6 presents a comparison of properties in silicon nitride samples fabricated by different additive manufacturing processes. While the density achieved in sintered samples fabricated by the CODE process was highest while comparing to other methods, i.e., robocasting, digital light printing, and inkjet printing, it should be noted that the other additive manufacturing processes did not use pressure less sintering for their fabricated parts; hot isostatic pressing, spark plasma sintering and gas pressure sintering methods were used. The CODE process combined with the pressureless sintering route was able to achieve the near theoretical density in the sintered samples. The fracture toughness in the CODE fabricated samples were found comparable to hardness values achieved in samples

fabricated by the stereolithography process. The sintering process for the CODE fabricated samples were carried out at a pressure of 0.1 MPa in nitrogen gas, the samples fabricated by stereolithography were sintered at a nitrogen gas pressure of 5 MPa. According to the densification reaction of silicon nitride, a high gas pressure favors densification and avoids any decomposition of silicon nitride. The hardness values achieved in silico nitride samples fabricated by the CODE process were the second highest, next to the hardness achieved by the digital light printing method which used HIP as the densification method. Conclusively, it could be observed that superior properties in CODE fabricated silicon nitride samples were achieved in comparison to other additive manufacturing methods which used less efficient/productive routes for sintering or densification [27].

Table 6. Comparison of properties found in silicon nitride additive manufacturing process

Method	**Density (%)**	**Hardness (GPa)**	**Fracture Toughness ($MPa.m^{1/2}$)**	**Reference**
Robocasting	98.6	N.A.	N.A.	[14]
Stereolithography	95.0	14.6 ± 0.45	5.8 ± 0.42	[16]
Digital Light Printing (DLP)	97.9	16.5	4.5	[17]
Inkjet 3D Printing	97.0	17	4.4	[18]
Binder jetting	70.0	N.A.	N.A.	[19]
Selective Laser melting (SLM)	82.0	11.8	N.A.	[20]
CODE (Ceramic On-Demand Extrusion)	~99.0	16.4 ± 1.1	5.5± 0.49	

4. CONCLUSION

In the manuscript, a study toward fabricating highly dense silicon nitride specimens using the ceramic on-demand extrusion (CODE) process, followed by pressureless sintering of the fabricated green parts was presented. Experimental analysis was used to

determine the optimal dispersant and binder contents for the formulation constituents for desired rheological properties. The CODE process parameters were tuned experimentally and systematically based on the first principles. Temperature vs. time profiles for debinding and sintering were established based on the result of thermogravimetric analysis and silicon nitride's sintering temperature. These together allowed us to achieve an average density of 99% in the silicon nitride specimens fabricated by the CODE process followed by pressureless sintering. The hardness measurements conducted showed the hardness value in the range of 1537-1755 kg/mm^2, which is comparable to the sintered silicon nitride achieved by traditional processes. The average fracture toughness of 5.5±0.49 MPa$\sqrt{m}$ achieved is comparable to the traditionally achieved fracture toughness in pressureless sintered silicon nitride specimens. The XRD analysis showed a transformation of α silicon nitride to β silicon nitride phase, which is favorable for achieving high-strength silicon nitride specimens.

ACKNOWLEDGMENT

The authors are grateful for the research funding by the Honeywell Federal Manufacturing & Technologies, LLC operates the Kansas City National Security Campus for the United States Department of Energy / National Nuclear Security Administration under Contract Number DE-NA0002839, and by the Innovative Smart & Additive Manufacturing (ISAM) laboratory at the Missouri University of Science and Technology.

REFERENCES

1. https.//www.colliercountyfl.gov/home/showpublisheddocument/91076/637165136542700000

2. Ghazanfari, Amir, Wenbin Li, Ming C. Leu, and Gregory E. Hilmas. "A Novel Freeform Extrusion Fabrication Process for Producing Solid Ceramic Components with Uniform Layered Radiation Drying." Additive Manufacturing 15, no. C (2017). 102-112.

3. Li, Wenbin, Amir Armani, Devin McMillen, Ming Leu, Gregory Hilmas, and Jeremy Watts. "Additive Manufacturing of Zirconia Parts with Organic Sacrificial Supports." International Journal of Applied Ceramic Technology 17, no. 4 (2020). 1544-1553.

4. Ghazanfari, Amir, Wenbin Li, Ming Leu, Jeremy Watts, and Gregory Hilmas. "Mechanical Characterization of Parts Produced by Ceramic on-demand Extrusion Process." International Journal of Applied Ceramic Technology 14, no. 3 (2017). 486-494.

5. Bocanegra-Bernal, M. H. and B. Matovic. "Mechanical Properties of Silicon Nitride-Based Ceramics and its use in Structural Applications at High Temperatures." Materials Science & Engineering. A Structural Materials. Properties, Microstructure and Processing 527, no. 6 (2010). 1314-1338.

6. Matovic B. Low-temperature sintering additives for silicon nitride. Max Planck Institute for Metals Research; 2003.

7. Zhao, Santuan, Wei Xiao, Mohamed N. Rahaman, David O'Brien, Jacob W. Seitz-Sampson, and B. Sonny Bal. "Robocasting of Silicon Nitride with Controllable Shape and Architecture for Biomedical Applications." International Journal of Applied Ceramic Technology 14, no. 2 (2017). 117-127.

8. S. C. Ventura et al., "Direct Photo Shaping-A New SFF Process for Ceramic Components, “Proceedings of the 71" International Conference on Rapid Prototyping, (1997), pp. 271-278.

9. Yang, J.-F., Ohji, T. and Niihara, K. (2000), Influence of Yttria–Alumina Content on Sintering Behavior and Microstructure of Silicon Nitride Ceramics. Journal of the American Ceramic Society, 83. 2094-2096.

10. Pashias, N., D. V. Boger, J. Summers, and D. J. Glenister. "A Fifty Cent Rheometer for Yield Stress Measurement." *Journal of Rheology (New York. 1978)* 40, no. 6 (1996). 1179-1189.

11. K. Hamad, M. Kaseem and F. Deri, "Melt Rheology of Poly (Lactic Acid)/Low Density Polyethylene Polymer Blends," *Advances in Chemical Engineering and Science*, Vol. 1 No. 4, 2011, pp. 208-214.

12. Othman, Norhayani. 2012. “Rheology and Processing of Poly (Lactides) and Their Enantiomeric Copolymers and Blends.” Electronic Theses and Dissertations (ETDs) 2008+. T, University of British Columbia.

13. Sarin, V. K. "On the α-to- β Phase Transformation in Silicon Nitride." Materials Science & Engineering. A, Structural Materials. Properties, Microstructure and Processing 105, no. 1 (1988). 151-159.

14. Zhao, Santuan, Wei Xiao, Mohamed N. Rahaman, David O'Brien, Jacob W. Seitz-Sampson, and B. Sonny Bal. "Robocasting of Silicon Nitride with Controllable Shape and Architecture for Biomedical Applications." International Journal of Applied Ceramic Technology 14, no. 2 (2017). 117-127.

15. Walish, J., Sutaria, M., Dougherty, M., Vaidyanathan, R., Peng, J., Calvert, P. and Cooper, K. (2000). Application of Design of Experiments to Extrusion Freeform Fabrication (EFF) of Functional Ceramic Prototypes. In 24th Annual Conference on Composites, Advanced Ceramics, Materials, and Structures. A. Ceramic Engineering and Science Proceedings (eds T. Jessen and E. Ustundag).

16. Liu, Yao, Lijin Cheng, Hao Li, Qing Li, Yuan Shi, Fei Liu, Qiu-mei Wu and Shaojun Liu. “Formation mechanism of stereolithography of Si3N4 slurry using silane coupling agent as modifier and dispersant.” Ceramics International 46 (2020). 14583-14590.

17. Ventura SC, Narang SC, Sharma S, Stotts J. A new solid freeform fabrication process for functional ceramic components. Solid Freeform Fabrication Symp. Proc. 1996.

18. Cappi, B., E. Özkol, J. Ebert, and R. Telle. "Direct Inkjet Printing of Si3N4. Characterization of Ink, Green Bodies and Microstructure." Journal of the European Ceramic Society 28, no. 13 (2008). 2625-2628.

19. Ripetskiy, Andrey A., Veniamin A. Pogodin, Sergey A. Sitnikov, Yury O. Solyaev, and Lev N. Rabinskiy. "Binder Jetting of Si3N4 Ceramics with Different Porosity." Solid State Phenomena 269, (2017). 37-50.

20. Minasyan, Tatevik, Le Liu, Marina Aghayan, Lauri Kollo, Nikhil Kamboj, Sofiya Aydinyan, and Irina Hussainova. "A Novel Approach to Fabricate Si3N4 by Selective Laser Melting." Ceramics International 44, no. 12 (2018). 13689-13694.

21. ASTM C373, Standard Test Method for Water Absorption, Bulk Density, Apparent Porosity, and Apparent Specific Gravity of Fired Whiteware Products, Ceramic Tiles, and Glass Tiles.

22. ASTM C1327, Standard test method for Vickers indentation hardness of advanced ceramics, West Conshohocken, PA. http.//dx.doi.org/10.1520/C1327, 2015.

23. ASTM C1421, Standard test methods for determination of fracture toughness of advanced ceramics, West Conshohocken, PA. http.//dx.doi.org/10.1520/C1421, 2007.

24. Ghazanfari, Amir, Wenbin Li, Ming C. Leu, Jeremy L. Watts, and Gregory E. Hilmas. "Additive Manufacturing and Mechanical Characterization of High Density Fully Stabilized Zirconia." Ceramics International 43, no. 8 (2017). 6082-6088.

25. Schneider, Caroline A., Wayne S. Rasband, and Kevin W. Eliceiri. "NIH Image to ImageJ. 25 Years of Image Analysis." Nature Methods 9, no. 7 (2012). 671-675.

26. MENDELSON, MEL I. "Average Grain Size in Polycrystalline Ceramics." Journal of the American Ceramic Society 52, no. 8 (1969). 443-446. 443–446.

27. https.//www.ceramics.net/sites/default/files/silicon_nitride_white_paperv9.pdf

28. Huang, Zheng Ren, Xiao Yang, Xue Jian Liu, Zheng Jiao, and Lu Jie Wang. "Effects of Particle Size on Densification Behavior of Si3N4 Ceramics." Key Engineering Materials 697, (2016). 182-187.

29. https.//www.azom.com/article.aspx?ArticleID=11076

30. https.//www.syalons.com/resources/articles-and-guides/silicon-nitride-ceramics.

31. HE, GUOPING; HIRSCHFELD, DEIDRE A. & CESARANO III, JOSEPH. Processing and mechanical properties of silicon nitride formed by robocasting aqueous slurries, article, January 26, 2000, Albuquerque, New Mexico. (https.//digital.library.unt.edu/ark./67531/metadc707231/. accessed October 12, 2021), University of North Texas Libraries, UNT Digital Library, https.//digital.library.unt.edu; crediting UNT Libraries.

32. Branko Matovic, Low Temperature Sintering Additives for Silicon Nitride, Dissertation an der Universität Stuttgart, Bericht Nr. 137 August 2003.

33. Lee, Dong-Duk, Suk-Joong L. Kang, Gunter Petzow, and Duk N. Yoon. "Effect of α to β (β') Phase Transition on the Sintering of Silicon Nitride Ceramics." Journal of the American Ceramic Society 73, no. 3 (1990). 767-769.

34. https.//www.pickpm.com/design-resource-center/typical-powder-metallurgy-parts/

35. https://www.materials.sandvik/en/products/hot-isostatic-pressed-hip-products/

36. Trice, Rodney W. and John W. Halloran. "Elevated-Temperature Mechanical Properties of Silicon Nitride/Boron Nitride Fibrous Monolithic Ceramics." Journal of the American Ceramic Society 83, no. 2 (2000). 311-316.

37. Greil, Peter, Ralf Nitzsche, Hannelore Friedrich, and Waldemar Hermel. "Evaluation of Oxygen Content on Silicon Nitride Powder Surface from the Measurement of the Isoelectric Point." Journal of the European Ceramic Society 7, no. 6 (1991). 353-359.

38. Lim, Woo-Sub, Jae-Wook Choi, Yusaku Iwata, and Hiroshi Koseki. "Thermal characteristics of hydroxypropyl methyl cellulose." Journal of Loss Prevention in the Process Industries 22, no. 2 (2009). 182-186.

SECTION

2. CONCLUSIONS AND RECOMMENDATIONS

2.1. CONCLUSIONS

This paper has discussed our study toward fabricating highly dense silicon nitride specimens using the ceramic on-demand extrusion (CODE) process, followed by pressureless sintering of the fabricated green parts. Experimental analysis was used to determine the optimal dispersant and binder contents for the formulation constituents for desired rheological properties. The CODE process parameters were tuned experimentally and systematically based on the first principles. Temperature vs. time profiles for debinding and sintering were established based on the result of thermogravimetric analysis and silicon nitride's sintering temperature. These together allowed us to achieve an average density of 99% in the silicon nitride specimens fabricated by the CODE process followed by pressureless sintering. The hardness measurements showed the hardness value in the range of 1537-1755 kg/mm^2, which is comparable to the sintered silicon nitride achieved by traditional processes. The average fracture toughness of 5.5±0.49 MPa$\sqrt{m}$ achieved is comparable to the traditionally achieved fracture toughness in pressureless sintered silicon nitride specimens. The XRD analysis showed a transformation of α silicon nitride to β silicon nitride phase, which is favorable for achieving high-strength silicon nitride specimens.

2.2. RECOMMENDATIONS

Critical to the paste formulation are. (i) particle size distribution of the powder. a widespread in particle size distribution promotes high green body density, which ultimately helps densification during sintering, (ii) homogeneity. homogeneity of the paste affects the dimensional consistency, and higher homogeneity reduces chances of formation of macro and micro cracks. The critical considerations to fabricating the parts by CODE process are. (i) The pneumatic pressure should be applied according to the calculated/measured values to avoid deviations/variations in the extrusion width of extruded filaments during the printing process, as the mismatch in paste input flow rate and paste extrusion flow rate will cause bulging in/bulging out of paste filament without an exception, (ii) The extrusion rate should always be equal to or higher than the traverse speed to achieve the maximum green body density in fabricated parts, (iii) overflow of oil over the top surface should be strictly avoided to produce parts without any delamination (iv) viscosity and solids loading of pastes needs to be in a carefully controlled range, very high viscosities and solids loading may result in delamination and cracks during fabrication process or while bulk drying of the green part.

APPENDIX

1. CODE PROCESS MODEL AND CONTROL

The control of parameters involved in the CODE process is very crucial for establishing the CODE process as a reliable industrial technology for continuously fabricating parts with minimum supervision and consistent mechanical properties and dimensional control. To make it possible, the CODE process control parameters can be categorized as controlling the following aspects of the CODE process. (i) paste rheology, (ii) paste homogeneity, (iii) part fabrication parameters (iv) parameters of densification, and (v) dimensional accuracy and control parameters.

1.1. PASTE RHEOLOGY

The paste rheology, which is majorly defined by the elastic shear modulus (G' (Pa)), viscous shear modulus (G" (Pa)), yield strength (σ) and viscosity (η) affects the performance of the fabrication process, the mechanical properties and dimensional accuracy and control of fabricated parts. The extrusion of paste becomes very difficult (pneumatic pressure of >80 psi unable to extrude out paste) when the elastic shear modulus (G') exceeds the value of G'> ~250,000 Pa. When the G' values are relatively lower (G'< 4000 Pa), the printed layers are unable to retain shape while being under the weight of the next layers of the green part. Thus, an optimum range of values for G'(Pa) is sought to extrude the paste at practically feasible pneumatic pressures (30 psi < P < 80 psi) while retaining the shape and dimensional control in deposited layers. Similarly, a suitable value of yield strength was sought to fabricated green parts without any slumping. The viscosity and shear viscous modulus are closely related to each other, the optimum viscosity in the

paste was also sought to avoid over extrusions due to low viscosity ($\eta < 500$ Pa. s) and avoiding high start delays due to very high viscosity ($\eta > 10,000$ Pa. s).

All the above-mentioned rheological properties are controlled by the following parameters of paste. (i) Particle size distribution (ii) Solids loading (iii) pH level (iv) binder content (iv) dispersant content.

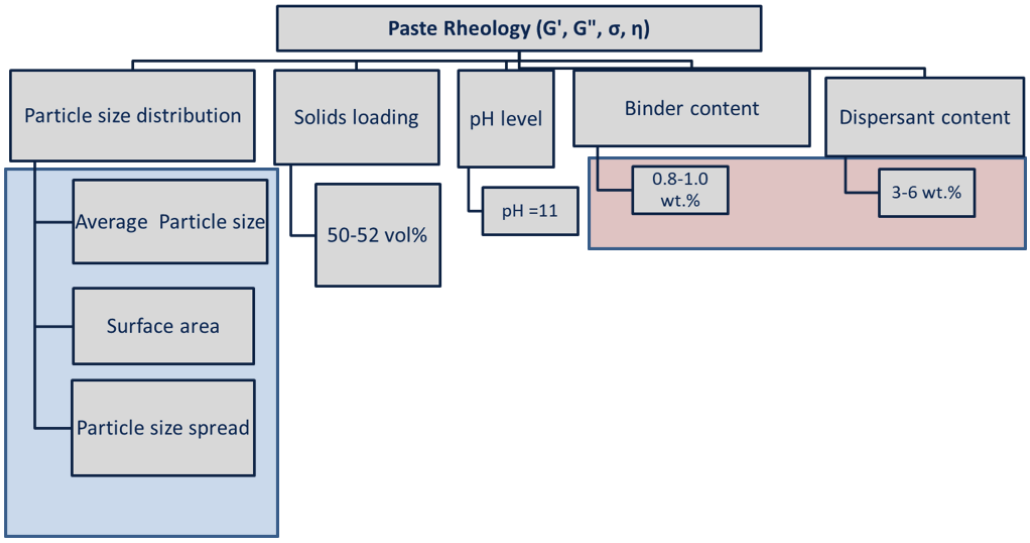

Figure A-1. Paste rheology and dependent factors

During the research effort on fabricating silicon nitride parts by CODE process, the suitable solids loading, and pH levels were established based on rheological tuning for crack-free, non-slumped, and uninterrupted green part fabrication. A range of binder content and dispersant content was established while tuning the rheology of the paste to match the rheology of polylactic acid (PLA) melts for fabricating parts with high dimensional control and accuracy. The sub-factors of the particle size distribution (marked by blue block) show that the particle size distribution is yet to be explored in the context

of its effect on rheology. Previous research had shown the existence of a relationship between the viscosity and dispersant's effectiveness with the sub-factors of particle size, surface area, and particle size spread.

1.2. PASTE HOMOGENEITY

The paste homogeneity is very important for the fabrication of porosity-free and crack-free parts along with the operation of the CODE process without any interruption due to nozzle blockages. The figure below describes the 5-step process for obtaining a homogeneous paste.

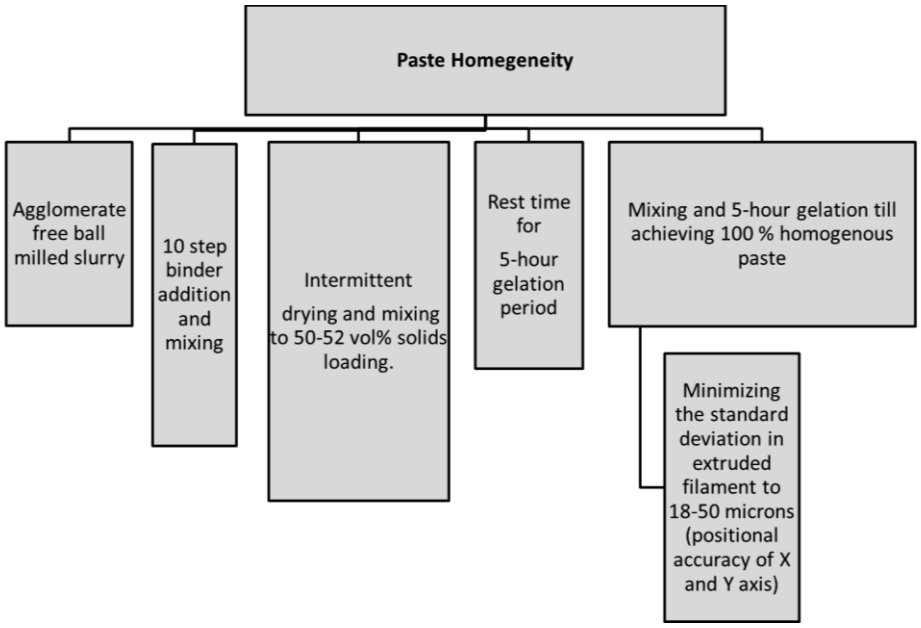

Figure A-2. Paste homogeneity

For future works, the 100% homogeneity of the paste can be confirmed if the standard deviation in the extrusion width in the extruded paste filament is below or equal to the positional accuracy (18-50 microns) of the X and Y-axis of the CODE machine.

1.3. PART FABRICATION PROCESS

One of the most important aspects of the CODE process is the fabrication process. To establish the CODE process as a reliable technology, the values of several major parameters were sought to be defined for fabricating green parts without any interruptions. The major fabrication parameters were. (i) layer height (ii) raster spacing (iii) start delay (iv) stop delay (v) extrusion speed and (iv) traverse speed.

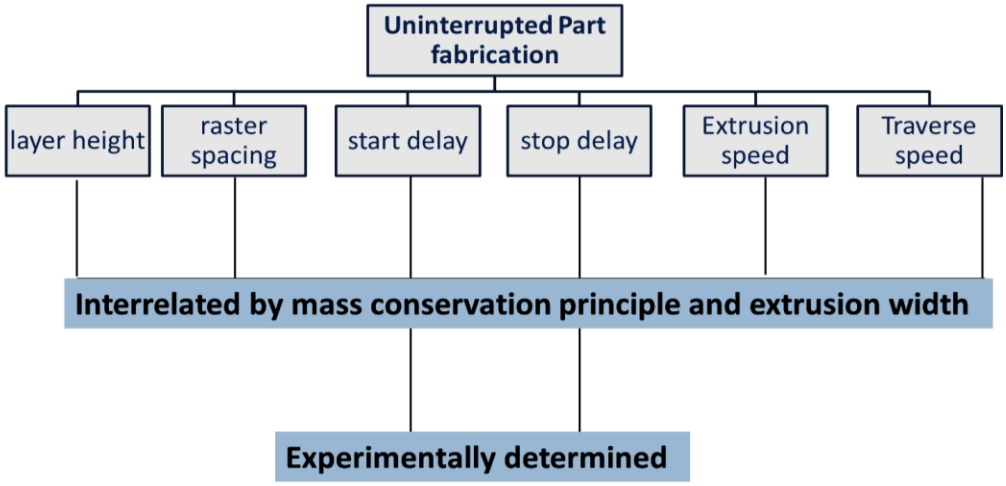

Figure A-3. Factors of part fabrication

Once the layer height is chosen by the user, the raster spacing can be determined by the measurement of extrusion width for a predetermined value of traverse speed by the use of mass conservation principle.

1.4. DENSIFICATION PROCESS

The densification process of the green sample is one of the main determinants of the final mechanical properties achieved in the sintered parts. The densification process

can be defined by the following factors. (i) binder burnout schedule (ii) sintering temperature (iii) sintering duration (iv) Powder bed composition (v) Nitrogen gas supply and (v) green density. As seen in the figure below, while temperature, duration, and nitrogen gas have been defined in the presented research. A close exploration of binder burnout schedule, the effect of powder bed composition on densification process, and the effect of particle size distribution and solids loading on green body density need attention for establishing tighter process control.

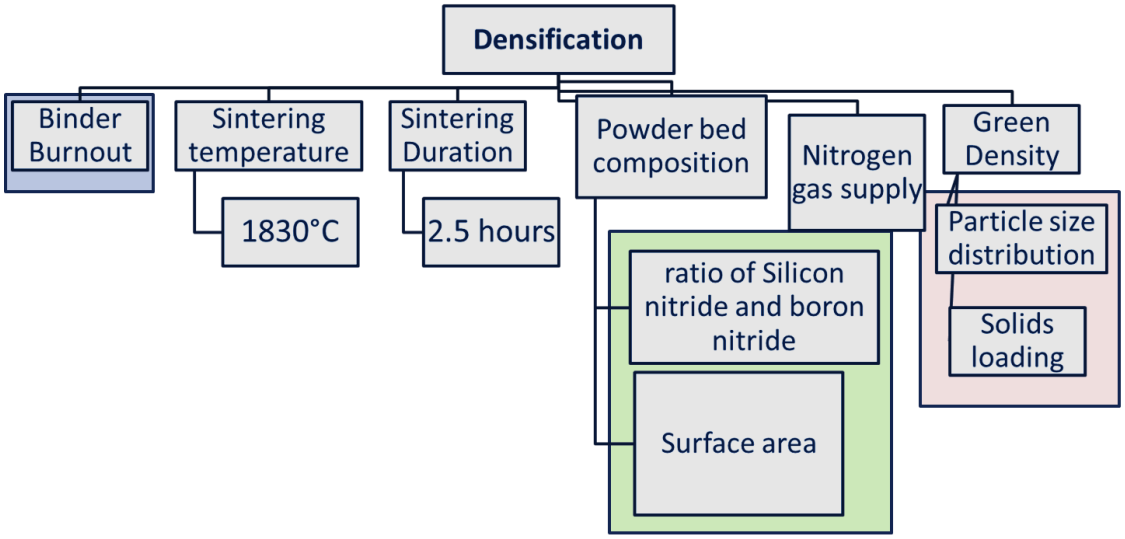

Figure A-4. Factors influencing densification behaviors

VITA

Sachin Choudhary was born in Bihar, India. He received his Bachelor of Technology in Mechanical Engineering from National Institute of Technology (NIT), Kurukshetra (India) in May 2014. Sachin Choudhary worked for MSIL (SUZUKI's joint venture with India's largest passenger car manufacturer) as an assistant manager in chassis research and development department. He later worked for two years at Oceaneering International, serving clients like Universal Studios and Disneyland as an engineering analyst. Sachin joined the Innovative Smart & Additive Manufacturing (ISAM) laboratory at Missouri University of Science and Technology (Missouri S&T) in Spring 2019 and started working on building the Ceramic On Demand Extrusion (CODE) Machine for additive manufacturing of ceramics and on the development of additive manufacturing method for silicon nitride. During his master research, he developed a method to fabricate ceramic parts with CODE process for fabricating parts with high complexity and near theoretical density, with comparable mechanical properties. In December 2021, he received his Master of Science in Mechanical Engineering under the direction of Dr. Ming C. Leu from Missouri University of Science and Technology, Rolla, Missouri, USA.